J Neurophysiol 109: 1548–1570, 2013.
First published December 12, 2012; doi:10.1152/jn.00237.2012.

Neural control of muscle force: indications from a simulation model

Paola Contessa[1,5] and Carlo J. De Luca[1,2,3,4]

[1]*NeuroMuscular Research Center, Boston University, Boston, Massachusetts;* [2]*Department of Electrical and Computer Engineering, Boston University, Boston, Massachusetts;* [3]*Department of Biomedical Engineering, Boston University, Boston, Massachusetts;* [4]*Department of Neurology, Boston University, Boston, Massachusetts; and* [5]*Department of Information Engineering, University of Padua, Padua, Italy*

Submitted 20 March 2012; accepted in final form 10 December 2012

Contessa P, De Luca CJ. Neural control of muscle force: indications from a simulation model. *J Neurophysiol* 109: 1548–1570, 2013. First published December 12, 2012; doi:10.1152/jn.00237.2012.—We developed a model to investigate the influence of the muscle force twitch on the simulated firing behavior of motoneurons and muscle force production during voluntary isometric contractions. The input consists of an excitatory signal common to all the motor units in the pool of a muscle, consistent with the "common drive" property. Motor units respond with a hierarchically structured firing behavior wherein at any time and force, firing rates are inversely proportional to recruitment threshold, as described by the "onion skin" property. Time- and force-dependent changes in muscle force production are introduced by varying the motor unit force twitches as a function of time or by varying the number of active motor units. A force feedback adjusts the input excitation, maintaining the simulated force at a target level. The simulations replicate motor unit behavior characteristics similar to those reported in previous empirical studies of sustained contractions: *1*) the initial decrease and subsequent increase of firing rates, *2*) the derecruitment and recruitment of motor units throughout sustained contractions, and *3*) the continual increase in the force fluctuation caused by the progressive recruitment of larger motor units. The model cautions the use of motor unit behavior at recruitment and derecruitment without consideration of changes in the muscle force generation capacity. It describes an alternative mechanism for the reserve capacity of motor units to generate extraordinary force. It supports the hypothesis that the control of motoneurons remains invariant during force-varying and sustained isometric contractions.

force model; muscle force; fatigue; firing rate; force twitch

THE CONTROL OF MOTOR UNIT firings and the regulation of muscle force during isometric contractions have been the subject of inquiry and controversy for decades. In this work, we develop a force model based on the latest physiological findings of motor unit firing behavior and on the time- and force-dependent changes in the muscle force generation capacity during isometric contractions.

Conflicting findings have been reported on the behavior of the firing rate and recruitment properties of motor units during isometric constant-force contractions, and various neurophysiological explanations have been proposed. The earliest reports by Person and Kudina (1972) and De Luca and Forrest (1973) found that the firing rates of motor units decrease during short (8–12 s) submaximal constant-force contractions. For contractions sustained longer, and up to the endurance limit, most studies report a subsequent increase in the firing rates of the active motor units accompanied by recruitment of new motor units (Adam and De Luca 2005; De Ruiter et al. 2004; Dorfman et al. 1990; Shimizu 1990). In contrast, studies by Christova and Kossev (2001) and Kuchinad et al. (2004) report a decrease in firing rates throughout sustained contractions. A more intricate behavior is reported by Garland et al. (1994, 1997), who describe increased firing rates for later-recruited motor units and decreased firing rates for earlier-recruited motor units during a fatiguing protocol. A more complex behavior is reported by Carpentier et al. (2001), who describe a steady decrease in the firing rates of earlier-recruited motor units, whereas later-recruited motor units first increase and subsequently decrease their firing rate.

Various explanations have been offered for these diverse characterizations of the firing rates, such as the "late adaptation" phenomenon reported by Kernell (1965a) or a combination of motoneuron adaptation and reflex inhibition along with spindle disfacilitation (Carpentier et al. 2001; Christova and Kossev 2001; Garland et al. 1994, 1997).

De Luca (1979) and De Luca et al. (1996) hypothesized that the early decrease was a consequence of the requirement to maintain the target force constant as the amplitude of the force twitches increased (potentiated) in the early part of the contraction, an explanation also advanced by Shimizu (1990). In a later work, Adam and De Luca (2005) proposed that the subsequent increase could be explained by an excitatory increase to the motoneuron pool as the muscle fatigues, an explanation also put forth by Dorfman et al. (1990) and De Ruiter et al. (2004).

In this work, we describe a muscle force model for testing the hypothesis that the firing rate behavior of motor units is a consequence of the different or altering motor unit force twitches to provide or maintain a target force. The model is not meant to replicate all the physiological processes involved in muscle force production, such as the electrochemical or mechanical processes that lead to spike initiation or muscle fiber contraction. It is intended to replicate the mechanism of producing an output muscle force that follows a given target force.

Of the various muscle force models reported in the literature, the majority do not include a feedback loop (see Fuglevand et al. 1993; Moritz et al. 2005; Taylor et al. 2002; Yao et al. 2000; Zhou and Rymer 2004; Zhou et al. 2007). The model of Lowery and Erim (2005) incorporates a feedback loop but for its intended purpose was not required to account for time-dependent changes in the motor unit force twitches. The most recent model provided by Dideriksen et al. (2010, 2011) contains both the force feedback loop and a description of time-varying muscle force but partially imposes time-depen-

Address for reprint requests and other correspondence: P. Contessa, NeuroMuscular Research Center, 19 Deerfield St., Boston, MA 02215 (e-mail: contessa@bu.edu).

dent behavior of the force fluctuations and of the excitatory drive to the motoneuron pool during sustained contractions.

In our model, the excitation to the motoneuron pool responds exclusively to changes in the mechanical requirement of the muscle. Thus our model differs from existing models, with the capability of simulating sustained force-tracking tasks with no other time-varying constraint on the system behavior than the empirically derived time-dependent adjustments in the muscle force twitch. In doing so, the model is able to replicate the following motor unit behaviors that have been previously reported during sustained contractions: *1*) the initial decrease and subsequent increase of the firing rates, *2*) the occasionally observed derecruited motor units during the early phase (~30–60 s) of a contraction, *3*) the recruitment of higher-threshold motor units as a contraction is sustained for longer periods of time, and *4*) the increasing force fluctuations as contraction time increases, and it provides *5*) an alternative explanation for the reserve capacity of motor units that is credited with supramaximal levels of force production. These results are obtained exclusively in response to the modeled time-varying muscle mechanical response, indicating that the force twitch characteristics are a dominant, although commonly overlooked, factor determining the firing rate behavior and the characteristics of the muscle force during isometric contractions.

METHODS

The basic notion is that the net excitation adjusts to compensate for the mechanical changes of the muscle fibers, implemented in the model as changes in the amplitude of the motor unit force twitches, via a feedback loop. The model has four fundamental components that are laid out in Fig. 1 and described herein.

Common drive (input excitation). The net excitation (φ), represented in Fig. 1*A*, consists of the sum of all excitatory and inhibitory inputs to the motoneuron pool and is common to all the motor units in the pool, according to the "common drive" property described by De Luca et al. (1982b) and De Luca and Erim (1994). It represents the average excitation required to attain a certain force level. In the absence of excitation ($\varphi = 0$), there is no active motor unit and no force is produced. During a force-varying isometric contraction, the force generated by the muscle is monotonically related to the net excitation. If the excitation is increased, additional motor units are recruited, and the firing rates of the active motor units and the force output increase. The maximal level of excitation ($\varphi = 1$) is the excitation required to exert the maximal force output.

Firing rate spectrum. The firing rate spectrum (Fig. 1*B*) is a set of equations developed by De Luca and Hostage (2010) and De Luca and Contessa (2012) that describes the firing rate behavior of motor units as a function of increasing net excitation to the motoneuron pool. It reflects both central and peripheral inputs, because it was derived from the analysis of motor unit firings during voluntary isometric contractions at increasing force levels where the central nervous system (CNS) and peripheral nervous system (PNS) jointly regulate motoneuron activation and the increase in muscle force. The firing rate spectrum formulates the "onion skin" property reported by De Luca et al. (1982a) and De Luca and Erim (1994). It describes a hierarchical inverse relationship between the recruitment threshold and the firing rate values of motoneurons at any time and force during a contraction. De Luca and Contessa (2012) derived the following exponential equation for the firing rate values of motor units as the excitation to the motoneuron pool increases from 0 to maximal levels in the first dorsal interosseous (FDI) muscle:

$$\lambda_i(\varphi, \tau_i) = 21 + 6.9\varphi - (23 + 85e^{-\frac{\varphi}{0.3}})\tau_i - e^{\frac{(\tau_i-\varphi)}{0.19\tau_i+0.05}} \times [9.8 + 6.9\varphi + (-8.7 - 85e^{-\frac{\varphi}{0.3}})\tau_i] \quad (1)$$

and in the vastus lateralis (VL) muscle:

$$\lambda_i(\varphi, \tau_i) = 19 + 8.0\varphi - (21 + 116e^{-\frac{\varphi}{0.2}})\tau_i - e^{\frac{(\tau_i-\varphi)}{0.16\tau_i+0.04}} \times [9.9 + 8.0\varphi + (-14.7 - 116e^{-\frac{\varphi}{0.2}})\tau_i], \quad (2)$$

where φ is the normalized input excitation, with $0 < \varphi < 1$; λ_i is the firing rate value corresponding to the input excitation φ; and τ_i is the

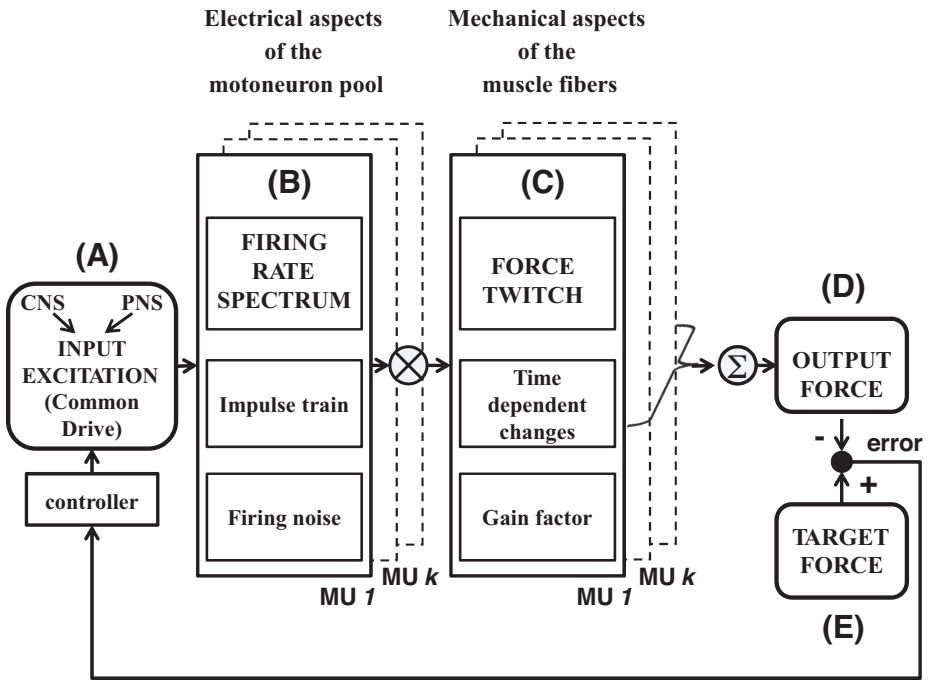

Fig. 1. Model schematic. The input to the muscle force model is the common net excitation to the motoneuron pool (*A*), which determines the "operating point" on the firing rate spectrum (*B*) and the firing rate values of the active motor units. These values are transformed into noisy firing trains, which are convolved with the time-dependent and firing rate-dependent motor unit force twitches (*C*) to compute the force contribution of each active motor unit. Motor unit forces are summed to obtain the muscle output force (*D*), which is compared with the target force (*E*). The tracking error between output and target force is used to adjust the input excitation. See text for additional details. MU, motor units.

recruitment threshold of the *i*th motor unit in the pool, with $0 < \tau_i < 0.67$ for the FDI, $0 < \tau_i < 0.95$ for the VL, and $\tau_{i+1} > \tau_i$. For additional details on the derivation of these equations, see APPENDIX A.

The firing rate spectrum is customized to a specific muscle by further specifying the motor unit threshold distribution, the recruitment range (τ_{max}) and the number of motor units (n) in the muscle. Specifically, for the FDI, $n = 120$ motor units (Feinstein et al. 1955) and the recruitment range is $\tau_{max} = 0–67\%$ maximum voluntary contraction (MVC) (De Luca and Hostage 2010). For the VL, $n = 600$ motor units (Christensen 1959) and $\tau_{max} = 0–95\%$ MVC (De Luca and Hostage 2010). The motor unit threshold distribution within the recruitment range is skewed to varying degrees for individual muscles, with the low-threshold motor units outnumbering the high-threshold motor units (Duchateau and Hainaut 1990; Milner-Brown et al. 1973). An equation for the motor unit threshold distribution for muscles consisting of varying numbers of motor units (MUs) and spindles was developed recently by De Luca and Kline (2012):

$$\%\text{active MUs} = 0.0058\, s\varphi(1 - 360e^{-5.9\varphi}) + 100(1 - e^{-9.8\varphi}) \quad (3)$$

where s (number of spindles) = 34 for the FDI muscle and $s = 440$ for the VL muscle.

In Fig. 2, the firing rate spectrum (*top*) and the distribution of recruitment thresholds (*bottom*) are presented for the FDI and VL muscles. The horizontal axis represents the input excitation, from zero to maximal. The set of trajectories in the spectra represents the firing rate pattern of motor units as a function of increasing excitation. Note that, for the sake of clarity, one of every six motor units is presented for the VL, and one of every two motor units is presented for the FDI. The vertical red line represents the "operating point," or the level of excitation to the motoneuron pool, set at 40% as an example. The operating point traverses the values of the mean firing rates of all recruited motor units, located to the *left* of the spectrum and identified in blue. The firing rate trajectories to the *right*, identified in gray, are the potential mean firing rates of the active motor units along with those of the motor units available for recruitment when the excitation to the motoneuron pool increases.

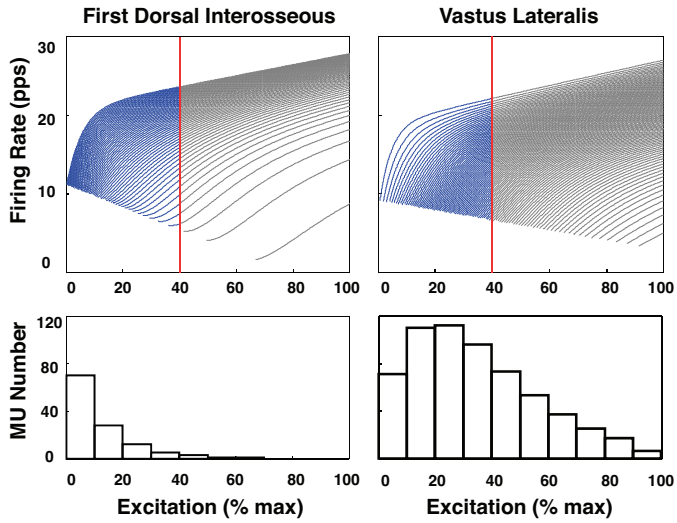

Fig. 2. *Top*: firing rate spectrum of the first dorsal interosseous (FDI) and vastus lateralis (VL) muscles showing the mean firing rate values (in pulses per second, pps) of the motor units as a function of the excitation to the motoneuron pool and the motor unit recruitment threshold. The red vertical line indicates a given level of input excitation or "operating point" of the motoneuron pool. It intersects the firing rate trajectories of the active motor units (displayed in blue) at the point of their average firing rate. The gray trajectories on the right side represent the potential firing rate values of motor units if the operating point of the muscles shifts to higher excitation levels. Note that the firing rates of only 1 of every 2 motor units (of 120) in the FDI and 1 of every 6 motor units (of 600) in the VL are displayed for clarity. *Bottom*: histogram of the recruitment thresholds (as a percentage of the maximal value, %max) for the motor units in the motoneuron pool of the FDI and the VL muscles. The range of recruitment threshold is from 0 to maximal (τ_{max}): $\tau_{max} = 67\%$ for the FDI and $\tau_{max} = 95\%$ for the VL.

Impulse train generator. The mean firing rate values of the active motor units, intercepted by the operating point in the firing rate spectrum, provide constant-frequency impulse trains for each active motor unit. Figure 3*A* shows 0.5-s impulse trains generated for five motor units of the FDI muscle (*motor units 1*, *30*, *60*, *90*, and *120*) when they are activated in response to 20% of maximal excitation (*top*) and in response to maximal excitation (*bottom*). Note that at 20% of maximal excitation, only *motor units 1–98* are active and the firing rate value is ~22.2, 20.1, 17.0, and 11.5 pulses per second (pps) for *motor unit 1*, *30*, *60*, and *90*, respectively. At maximal excitation, all available motor units are active and the firing rate value increases to 27.6, 27.1, 25.6, 21.3, and 9.9 pps for *motor units 1*, *30*, *60*, *90*, and *120*, respectively.

The firing instances in the impulse trains are then modified with the addition of synaptic noise (Fuglevand et al. 1993) by modeling the interpulse interval (IPI) between two adjacent firings of a motor unit as a random variable with Gaussian distribution and a coefficient of variation of 20% (Clamann 1969; Macefield et al. 2000; Moritz et al. 2005; Nordstrom et al. 1992). Other studies have reported that the IPIs of motor units have a skewed distribution (De Luca and Forrest 1973; Person and Kudina 1972). However, a Gaussian distribution is used here for the sake of simplification. The addition of noise in the 0.5-s impulse trains of Fig. 3*A* is depicted in Fig. 3*B*. For additional details see APPENDIX B.

Force twitch. The force twitch of a motor unit is an estimate of the force associated with a single motor unit action potential. It is commonly described with three parameters: the amplitude P, defined as the peak value; the rise time Tr, defined as the time from the beginning of the force twitch to the peak value; and the half-relaxation time Thr, the time from the peak value to the point where the amplitude is reduced to one-half of the peak value. The shape of the force twitch is mathematically generated with the equation developed by Raikova and Aladjov (2002) in which these three parameters may be adjusted independently:

$$f(t) = pt^m e^{-kt} \quad (4)$$

with

$$p = \mathrm{P}e^{-k\mathrm{Tr}(\log\mathrm{Tr}-1)} \quad (5)$$

$$m = k\mathrm{Tr} \quad (6)$$

$$k = \frac{\log 2}{\mathrm{Thr} - \mathrm{Tr}\log(\mathrm{Tr} + \mathrm{Thr}/\mathrm{Tr})} \quad (7)$$

Lower-threshold motor units generally produce lower-amplitude, longer-duration force twitches than higher-threshold motor units (Burke et al. 1973; Calancie and Bawa 1985; Henneman and Olson 1965; Milner-Brown et al. 1973; Monster and Chan 1977). Values of the twitch parameters for all the motor units in the muscle were taken from the literature for the FDI, whereas they were derived from our own empirical data for the VL. For additional details see APPENDIX C.

The set of modeled motor unit force twitches is presented in Fig. 4*A*. For the purpose of clarity, the force twitches of one of every two motor units are presented for the FDI muscle, and those of one of every six motor units are presented for the VL muscle. Note that the force twitch amplitude becomes greater and the time duration becomes shorter for progressively higher-threshold motor units. The distributions of the motor unit force twitch parameters are reported in Fig. 4*B* for the FDI and VL muscles.

Time-dependent modulation of the force twitch amplitude. It is generally accepted that the amplitude of the muscle force twitch increases at the beginning of a sustained contraction (potentiation) and subsequently decreases as fatigue progresses (Burke 1981; Dolmage

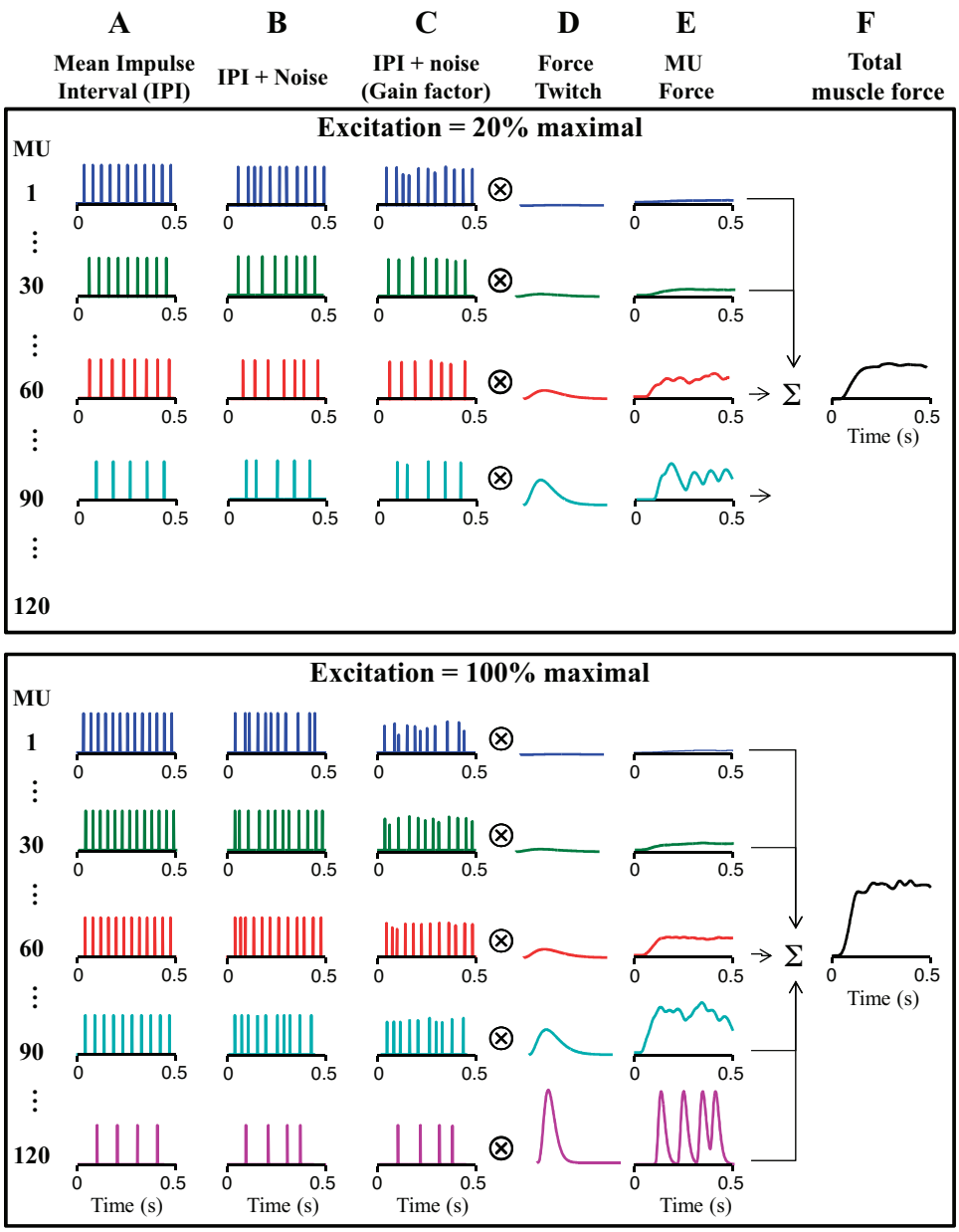

Fig. 3. *A*: impulse trains generated for *motor units 1*, *30*, *60*, *90*, and *120* in the FDI muscle during a 0.5-s isometric voluntary contraction sustained at 20% (*top*) and 100% (*bottom*) maximal excitation. IPI, interpulse interval. *B*: impulse trains modified with superimposed Gaussian noise, representing the synaptic noise. *C*: noisy impulse trains scaled on the basis of the firing rate-dependent gain function presented in *Eqs. 13* and *14*. *D*: motor unit force twitch. *E*: motor unit forces obtained by convolving the impulse trains in *C* with their respective force twitch in *D*. *F*: output muscle force generated from the summation of all motor units active in the FDI muscle at the set excitation level. Note that motor unit force twitches and motor unit forces of each muscle are on the same scale.

and Cafarelli 1991; Macintosh et al. 1994; Vandervoort et al. 1983). There is a lack of agreement in the literature as to the behavior of the duration of the force twitch during a sustained contraction. For instance, muscle force twitch duration was found to increase by Bigland-Ritchie et al. (1983), to decrease by Vøllestad et al. (1997), and to remain constant by Binder-MacLeod and MacDermond (1993). Therefore, in our simulations we varied only the amplitude of the motor unit force twitches as a function of contraction time, whereas the time duration was assumed to remain constant. Nonetheless, we explored the influence of increasing and decreasing force-twitch duration and found no noticeable effect on the simulated motor unit and muscle force behavior during repeated sustained contractions. Refer to APPENDIX D for details.

We calculated the time dependence of the amplitude of the motor unit force twitches on the basis of the time-dependent behavior of the evoked muscle force twitch obtained in our previous studies (Adam and De Luca 2003, 2005 for the VL; unpublished data for the FDI). In those studies, the muscle force twitch was recorded by electrically stimulating the FDI and VL muscles at supramaximal intensity in the rest periods between repeated isometric contractions sustained at 20% MVC. We found that the amplitude of the muscle force twitch increased by ~20% after 60 s in the FDI and by 10% after ~40 s in the VL. Afterward, the amplitude decreased approximately linearly to 40% of the initial value after 14 min in the FDI and to 60% of the initial value after 10 min in the VL. This time course is used to modulate the amplitude of the force twitches of the active motor units in the model: the amplitude is linearly increased in the first 60 s of the contraction in the FDI and in the first 40 s of the contraction in the VL, and it is later decreased linearly so that the amplitude of the simulated muscle force twitch, computed as the sum of all motor unit force twitches, shows values similar to those obtained in the studies of Adam and De Luca (2003, 2005). This time-dependent pattern of force change is applied to all motor units as a function of contraction time: the force twitches of the active motor unit potentiate only at the beginning of a contraction and subsequently decrease. Thus motor units recruited for the first time after 60 s (in the FDI) or 40 s (in the VL) will not show any potentiation, but their force twitch amplitude will diminish from recruitment. This choice was based on the lack of available data regarding the time-dependent changes in the force twitch of individual motor units during voluntary sustained con-

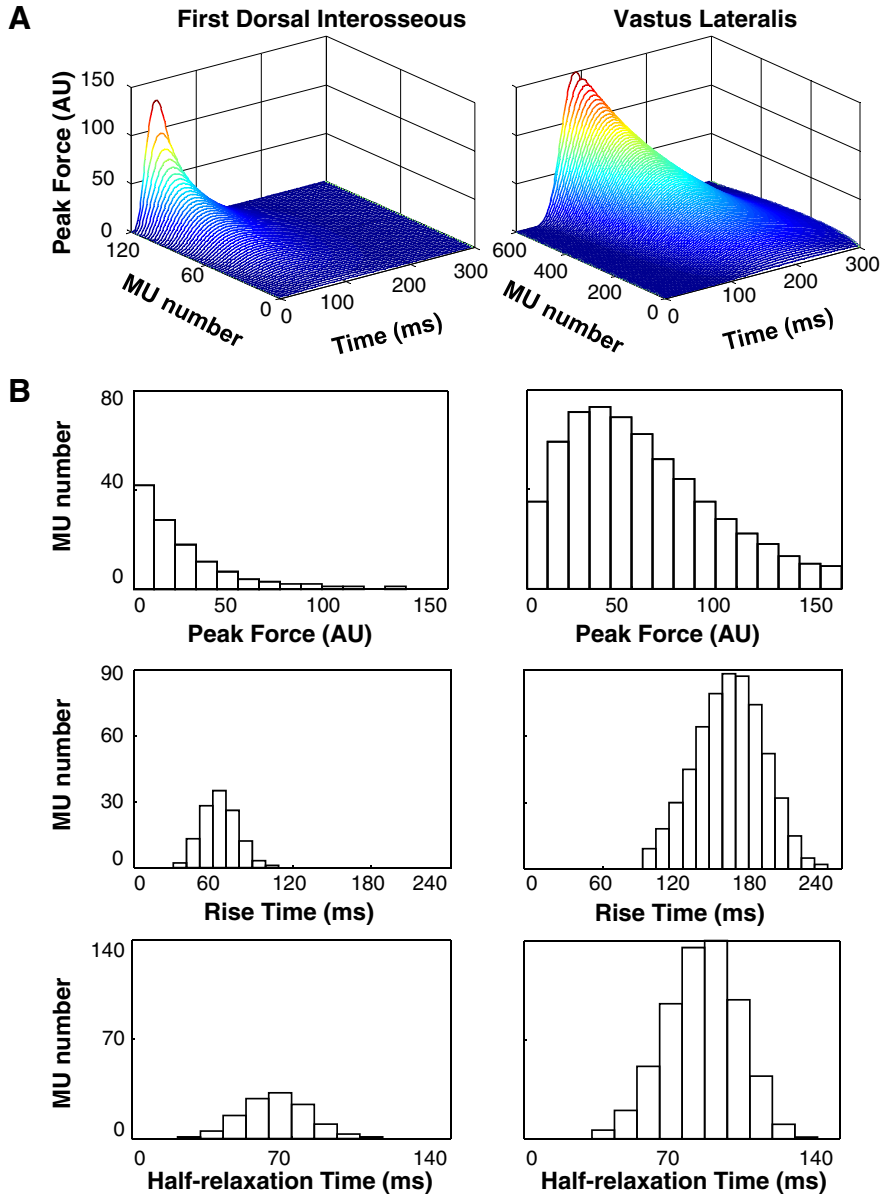

Fig. 4. *A*: force twitches modeled with *Eqs. 3–7* for motor units in the FDI and VL muscle. Note that the force twitches of only 1 of every 2 motor units in the FDI and 1 of every 6 motor units in the VL are displayed for clarity. Higher-threshold higher-amplitude motor units show progressively shorter time duration. AU,. arbitrary units. *B*: histograms of the 3 parameters characterizing the force twitch for the FDI and VL muscles: peak tension (force), rise time, and half-relaxation time.

tractions. The description of the time-dependent characteristics of the motor unit force twitches may be improved as more consistent and comprehensive data on individual motor units become available. However, the hypothesis that all motor units initially potentiate after recruitment is also plausible. We explored this condition in APPENDIX D.

It should also be noted that the time-dependent modulation adopted in this study is intended to mimic the modulation that occurred during the empirical protocol of Adam and De Luca (2003, 2005). Other protocols would likely produce different time-varying modulations. This amplitude modulation will serve to test the model by comparing the simulation output with the empirical data obtained by Adam and De Luca (2005). For additional details see APPENDIX D.

Firing rate-dependent gain factor. Experiments where motor units are stimulated at a fixed frequency have shown that the summation of force during tetanic contractions is nonlinear and depends on the stimulation rate (Bawa and Stein 1976; Cooper and Eccles 1930; Fuglevand et al. 1993; Mannard and Stein 1973). We obtained force-frequency curves by supramaximal stimulation of the VL (Adam and De Luca 2003, 2005) and FDI (unpublished data). The curves were fitted to exponential functions, following the procedure of Herbert and Gandevia (1999) and Studer et al. (1999), and divided by the stimulus rate to obtain a firing rate-dependent gain factor, which was then normalized for each motor unit on the basis of the rise time of the force twitch. The gain factor thus computed is used in the model to account for the nonlinear summation of twitches by scaling the amplitude of each motor unit pulse in the train of firings as a function of the corresponding IPI. The effect of the gain factor on the impulse trains of Fig. 3*B* is presented in Fig. 3*C*. For additional details see APPENDIX E.

Motor unit force. The force F_i generated by the *i*th motor unit in the muscle is computed by convolving the impulse train with the time-dependent force twitch, f_i. The force F_i is thus comprised of the sum of the time-shifted individual impulse responses:

$$F_i(t) = \sum_j f_{ij}(t - t_{ij}), \quad (8)$$

where t_{ij} is the *j*th firing time of motor unit *i* and f_{ij} is the force twitch of motor unit *i* at the time of the *j*th firing. The force outputs generated by *motor units 1*, *30*, *60*, *90*, and *120* in response to a 0.5-s-long excitation at 20% (*top*) and 100% (*bottom*) of maximal excitation are depicted in Fig. 3*E*.

Muscle force. The total muscle force, $F_{tot}(t)$, is obtained by summation of the forces produced by all active motor units (Fig. 1*D*). If k is the number of active motor units,

$$F_{tot}(t) = \sum_{k} F_k(t). \quad (9)$$

Finally, the force is low-pass filtered at a cutoff frequency of 5 Hz to account for the filtering effect of the muscle tissues. Figure 3*F* shows the force obtained from the summation of the individual forces of *motor units 1*, *30*, *60*, *90*, and *120* of the FDI in response to a 0.5-s excitation at 20% (*top*) and 100% (*bottom*) of maximum.

Feedback loop. The target force is divided into time intervals of length $dt = 0.5$ s. In each interval, the error in the simulated output force, consisting of the difference between the average force output (see Fig. 1*D*) and the average target force (see Fig. 1*E*), is calculated. If the error surpasses a predetermined threshold, which for this report is set at 5% of the target force value, the input excitation is adjusted proportionally and the simulation is repeated. If the error is negative, the excitation is increased; otherwise, the excitation is decreased. The simulation in each interval is repeated until the output force matches the target force within the 5% tolerance limit. When the error is within limits, the simulation proceeds to the following time interval. This procedure is represented in Fig. 1 by the box labeled "controller."

In each interval *dt*, the parameters of the model, such as the input excitation, the number of active motor units, and the amplitude of the motor unit force twitches, are kept at a constant value to reduce the computational time. The *dt* was set at 0.5 s so that its length could be small enough to allow physiological changes in the parameters with contraction time but also large enough to allow multiple firings for each motor unit and summation of force twitches to occur.

Simulation procedure. The model is implemented using Matlab and the Simulink tool. The simulation sampling time is set to 1 ms to allow accurate translation of the firing rates into impulse trains. The simulation proceeds as follows:

1) The MVC force value is obtained at the beginning of the simulation as the force produced when all motor units are activated at maximal excitation ($\varphi = 1$) and is used for calibrating the simulated output force (in %MVC).

2) The target force (in % MVC) is divided into time intervals of length $dt = 0.5$ s. During this increment the input excitation and all the parameters of the model are kept constant.

3) The initial input value of excitation φ in each interval *dt* is based on the value used in the previous interval. The starting value at the onset of a contraction is set to $\varphi = 0$.

4) The number of active motor units and their firing rate value at the input excitation is computed. For each motor unit, an impulse train of length *dt* is generated with a constant IPI equal to the inverse of the firing rate value. Each IPI is then modified to introduce firing rate variability and the firing rate-dependent gain factor.

5) For each motor unit, the noisy impulse train is convolved with the time-dependent force twitch f_i to generate the individual forces F_i, which are summed to obtain the total output force F in the current interval.

6) The average value of the force F is compared with the average value of the target force in the current interval. If the difference (tracking error) is within ±5% of the target force value, the simulation proceeds to the next interval; otherwise, the excitation is adjusted and *steps 4*, *5*, and *6* are repeated.

The simple force feedback is intended to regulate the input excitation and maintain the force output at the required target level, such as when the muscle force diverges from the target force during visually guided tracking tasks. Note that the force feedback implemented in the model does not introduce any delay that would be present in real conditions due to the time needed to process the visual error information and effectuate the corrective actions. This choice was made because the force feedback in the simulations presented is not meant to replicate any specific physiological feedback process (which would differ depending on the tracking modality) nor to address any latency at which these feedback processes would function. Instead, it is merely intended to reproduce its approximate end result, i.e., to maintain the simulated force at the target level by adjusting the excitation to the motoneuron pool regardless of the tracking modality, associated delay, or subject tracking ability.

A more realistic approach would involve the process of detecting an error between the output muscle force and the target force, processing the error information, and adjusting for this error with a delay, which is ~150 ms in the case of visual tracking tasks (Lowery and Erim 2005; Slifkin et al. 2000). To ensure that the introduction of a time delay in the feedback did not alter the pattern of the motor unit behavior, simulations were run by adjusting the excitation to the motoneuron pool at fixed intervals of 150 ms proportionally to the average tracking error in the previous interval. The gain of the force feedback was set to 0.1 for both muscles and was maintained constant with contraction time. At the end of the RESULTS, the results of these simulations are compared with the results of the simulations obtained with the above-mentioned feedback approach with no delay.

RESULTS

We simulated three force paradigms with the FDI and VL muscles. In the first paradigm, a constant excitation value producing an initial target force of 20% MVC was simulated in the absence of force feedback, to illustrate the need for a force feedback loop to maintain the force constant. In the second paradigm, force feedback was included in the model and the force output was maintained at a constant level of 20% MVC throughout the simulated contraction. In the third paradigm, the force output consisted of a series of repeated intermittent contractions, each first briefly rising to 50% MVC and subsequently decreasing to 20% MVC, where it was sustained for 50 s. This force paradigm mimicked the protocol of Adam and De Luca (2003, 2005) and allowed direct comparison of the simulated data with empirical observations. Last, we repeated the third paradigm using the modified force feedback, introducing a 150-ms delay for correcting the force tracking error, as detailed in METHODS.

Note that only the time-dependent change in the amplitude of the motor unit force twitches is predetermined in the model.

Contraction sustained at a constant excitation level with no feedback. Figure 5*A* for the FDI and 5*B* for the VL muscles present the results of the simulation of a contraction sustained at a fixed value of the input excitation to the motoneuron pool. A 60-s epoch at the onset of the sustained contraction is shown in Fig. 5, *A* and *B*, *top*; and a subsequent 60-s epoch taken well into the contraction (in this case at the 11th minute for the FDI and at the 4th minute for the VL) is shown in Fig. 5, *A* and *B*, *bottom*. The *left* panels show the firing rate spectrum of the muscles, with the red line indicating the value of the input excitation (or the operating point) during the presented epoch. The *middle* panels present the mean firing rates of the active motor units in the 60-s epoch, computed by low-pass filtering the impulse trains with a 2-s Hanning window. The mean firing rates of only one of every six motor units are shown for clarity in both muscles. In *right* panels, the red line represents the input excitation and the blue line represents the simulated output force. A magnified view of the output force is presented in the *insets*. Above each *right* panel, the muscle force twitch at the onset and at the end of the epoch is presented, computed as the sum of the force twitches of all motor units in the muscle

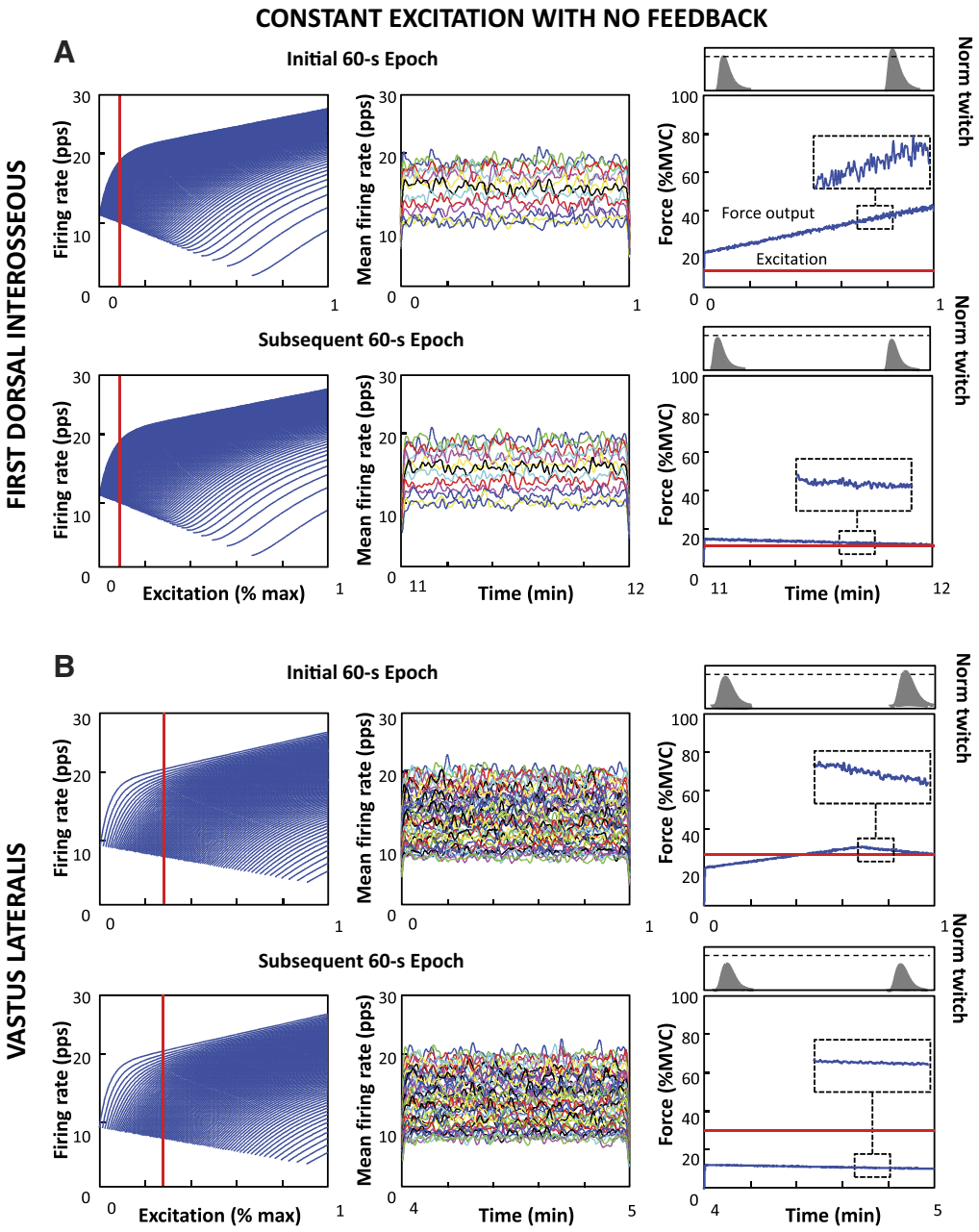

Fig. 5. *A* and *B*: initial 60-s epoch (*top*) and subsequent 60-s epoch (*bottom*) of a simulated contraction sustained at a constant excitation value for the FDI (*A*) and VL muscles (*B*). *Left* panels present the firing rate spectrum of the muscles; the red line indicates the value of input excitation, or the operating point. *Middle* panels contain the mean firing rates of the active motor units during the 60-s epochs. Only 1 of every 6 motor units is displayed for clarity. *Right* panels show the simulated output force (as a percentage of maximum voluntary contraction, %MVC) in blue and the input excitation in red. A 10-s enlarged view of the force is presented in the box *insets*. The whole muscle force twitch at the beginning and at the end of the epoch, with amplitude normalized to that at the beginning of the contraction, is presented in gray shading at the *top* of the *right* panels. In the absence of force feedback, the excitation to the motoneuron pool remains constant, as do the number of active motor units and their firing rate value. The muscle force twitch increases during the first 60 s or less as a result of potentiation, leading to increased simulated output force. It subsequently decreases as the contraction is sustained and the muscle fatigues, leading to a decrease in the simulated force output. Note that the simulated muscle force is smoother for the VL than for the FDI.

and with amplitude normalized to the value at the beginning of the contraction.

With no feedback available for regulating the input excitation, its value remained constant throughout the simulation in both muscles (see the red lines in Fig. 5, *A* and *B*, *left* and *right*), as did the number of active motor units and their mean firing rates. The model was not able to maintain the force at the constant target value: the output force increased during the first 60-s epoch in the FDI and during the first 40 s in the VL, and subsequently decreased until the endurance limit. Changes in the output muscle force followed the time-dependent adjustments in the muscle force twitch, whose amplitude also increased during the first 60 and 40 s and then decreased progressively to the endurance limit. The coefficient of variation of the force remained constant throughout the sustained contraction, indicating that the standard deviation of the force initially increased and then decreased with contraction time, as the muscle force also increased and then decreased. All these modulations were exclusively due to the modifications in the amplitude of the force twitches, the only parameter changing during the simulation. See Fig. 5 and Table 1 for details. Note that a greater initial excitation level was necessary to produce a 20% MVC force output in the VL than in the FDI because of the different mechanical properties and recruitment threshold distribution of the two muscles. For the same reasons, a similar decrease in simulated muscle force was obtained sooner in the VL than in the FDI; and the coefficient of variation of the force was greater in the FDI than in the VL.

Contraction sustained at a constant force level with feedback. Figure 6, *A* and *B*, presents the results of the simulation of the contraction sustained at a constant force level of 20% MVC with the enabled force feedback. Data are presented in a similar

Table 1. *Constant excitation/force*

	Contraction at Constant Excitation Level				Contraction at Constant Force Level			
	FDI		VL		FDI		VL	
	First epoch	Last epoch	First epoch	Last epoch	First epoch	Last epoch	First epoch	Last epoch
Epoch	1	12	1	5	1	17	1	16
Excitation at onset, %max	9.4	9.4	27.4	27.4	9.4	49.6	28.4	82.5
Excitation at end, %max	9.4	9.4	27.4	27.4	5.3	71.6	23.0	93.8
No. of active MUs at onset	68	68	265	265	68	118	276	582
No. of active MUs at end	68	68	265	265	44	120	206 (+12)	599
Average MU firing rate, pps	15.1 (9.9–19.6)	15.1 (9.8–19.8)	13.8 (7.3–21.0)	13.8 (7.5–21.1)	15.2 (11.9–18.5)	20.8 (5.5–24.8)	13.8 (8.2–20.7)	18.6 (5.2–26.0)
Force at onset, %MVC	19.9	13.0	20.0	11.2	20.1	20.3	20.2	20.3
Force at end, %MVC	45.2	10.1	27.4	9.2	19.9	19.8	19.4	19.8
Force CV, %	1.4	1.4	0.5	0.6	1.5	3.5	0.6	1.5
Normalized twitch at onset	1.00	0.93	1.00	0.92	1.00	0.49	1.00	0.39
Normalized twitch at end	1.26	0.90	1.07	0.90	1.16	0.38	1.06	0.33

Data are results of the simulations for the contractions performed at a constant excitation level and constant force level for the first dorsal interosseous (FDI) and vastus lateralis (VL) muscles (range is shown in parentheses for MU firing rate). %max, percentage of maximum; MUs, motor units; %MVC, percentage of maximal voluntary contraction; pps, pulses per second.

manner as in Fig. 5. The only difference is that two red lines are now present in the firing rate spectra in the *left* panels: the solid line indicates the value of the input excitation at the beginning of the 60-s epoch, and the dotted red line indicates the value of input excitation at the end of the 60-s epoch presented. The arrows indicate the direction of the excitation change during the time epoch. The first 60-s epoch and last 60-s epoch during which the target force could be maintained are presented in Fig. 6. In the following epoch, the excitation reached maximal level and the force production could not be sustained at the target level.

With feedback available, the model was able to maintain the force at the constant target value. The excitation required to sustain the 20% MVC force level decreased during the first 60-s epoch in the two muscles, shifting the operating point toward lower excitation levels and causing a decrease in the firing rates of the active motor units and derecruitment of several motor units. These adjustments occurred concurrently with an increase in the amplitude of the muscle force twitch, as shown in Fig. 6 at the *top* of the *right* panels. Twelve motor units were recruited again toward the end of the 60-s epoch in the VL muscle, where the peak of the potentiation phase occurred at 40 s. The contraction was maintained for over 17 min in the FDI and for over 16 min in the VL. After the first 60-s epoch the excitation required to sustain the same force level increased progressively with contraction time, shifting the operating point in the firing rate spectra toward higher excitation values. This phenomenon was accompanied by progressive increase in the firing rates of the active motor units and recruitment of additional motor units, and followed the progressive decrease in the amplitude of the muscle force twitch. The coefficient of variation of the force increased during the contraction. These modifications are presented in Fig. 6 and Table 1 for the last 60-s epoch that could be completed by the two muscles, i.e., *minute 16* to *17* in the FDI and *minute 15* to *16* in the VL. The simulations continued after the last epoch presented, but shortly after this point, the endurance limit was reached and the force could no longer be sustained at the target level. Note the increase in the range of motor unit firing rates by the last 60-s epoch: the lower minimum firing rate value indicates that additional higher-threshold lower-firing rate motor units were recruited; the higher maximum firing rate value indicates that the firing rate of the lower-threshold motor units, which were active from the beginning of the contraction, increased.

Repeated intermittent contractions with feedback. Figure 7, *A* and *B*, presents the results of the simulation of the repeated intermittent contractions for the FDI and VL muscle, respectively. Data are presented in a similar manner as in Figs. 5 and 6. The only difference is that the *top* and *bottom* panels of Fig. 7, *A* and *B*, do not correspond to 60-s epochs of a sustained contraction but to the first contraction and the last contraction before the endurance limit of the series of intermittent repeated contractions.

In both muscles and all contractions, a higher excitation value was necessary to exert the initial 50% MVC than the following 20% MVC muscle force output, which was associated with a lower number of active motor units and lower motor unit firing rates. During the 20% MVC plateau region of the first contraction, the input excitation required to maintain the target force decreased slightly in both muscles, shifting the

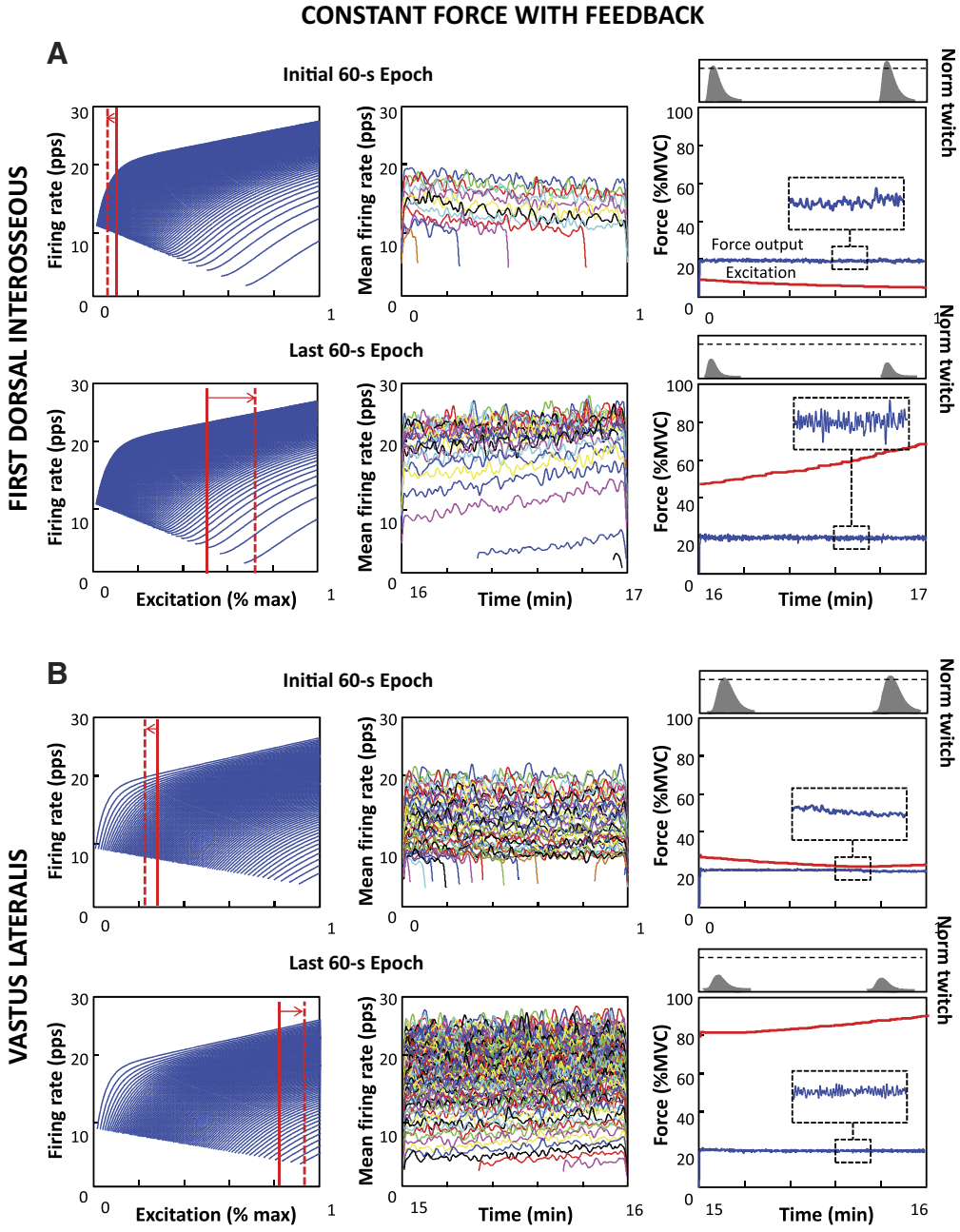

Fig. 6. *A* and *B*: simulated contraction sustained at a constant force value for the FDI (*A*) and VL muscles (*B*). The first 60-s epoch of the contraction (*top*) and the last 60-s epoch before the endurance limit (*bottom*) are presented. Data are presented in a similar manner as in Fig. 5. *Left* panels now present 2 red lines indicating the value of input excitation, or operating point, at the beginning (solid line) and at the end (dotted line) of the epochs. With force feedback, the excitation to the motoneuron pool decreases in the first 60-s epoch, following the increase in muscle force twitch amplitude and leading to decreased firing rates of the active motor units and derecruitment of several motor units. The opposite phenomena occur as the contraction is sustained longer and are presented for the last 60-s epoch before the endurance limit. The force remains at the constant target value throughout the simulation and presents a marked increase in force fluctuations.

operating point to the left of the firing rate spectrum and leading to decreasing firing rates of the active motor units and derecruitment of several motor units. Adjustments occurred concurrently with an increase in the muscle force twitch amplitude. Sixteen motor units were recruited again at the end of the plateau phase in the VL muscle, since the muscle force twitch reached its maximal amplitude at 40 s and then started to decrease. Note that the last motor unit to be derecruited was the first to be recruited again.

Throughout the series of repeated contractions, the input excitation needed to exert both the initial 50% MVC and subsequent 20% MVC force increased progressively with contraction time, shifting the operating point to the right of the firing rate spectra of both muscles. A progressively greater number of motor units were recruited and fired at increasing average firing rates. These adjustments were accompanied by a progressive decrease in the muscle force twitch amplitude and are presented in Fig. 7 and Table 2 for the first and last contraction of the series in both muscles. The coefficient of variation of the force increased with contraction time. The model simulated 14 sequential contractions for the FDI and 10 for the VL. At these points, the endurance limit was reached and the force could no longer be sustained at the target level. See Fig. 7 and Table 2 for details.

Although the emphasis has been on the motor unit time-varying behavior during the constant force plateau region sustained at 20% MVC, it is evident in Fig. 7 that increasing and decreasing forces can be simulated; witness the simulated force ramp up to 50% MVC, the decrease to 20% MVC, and the final decrease to 0% MVC. Figure 3, *A* and *B*, further shows that as the higher threshold motor units are recruited to generate increasingly greater forces, the force fluctuations increase.

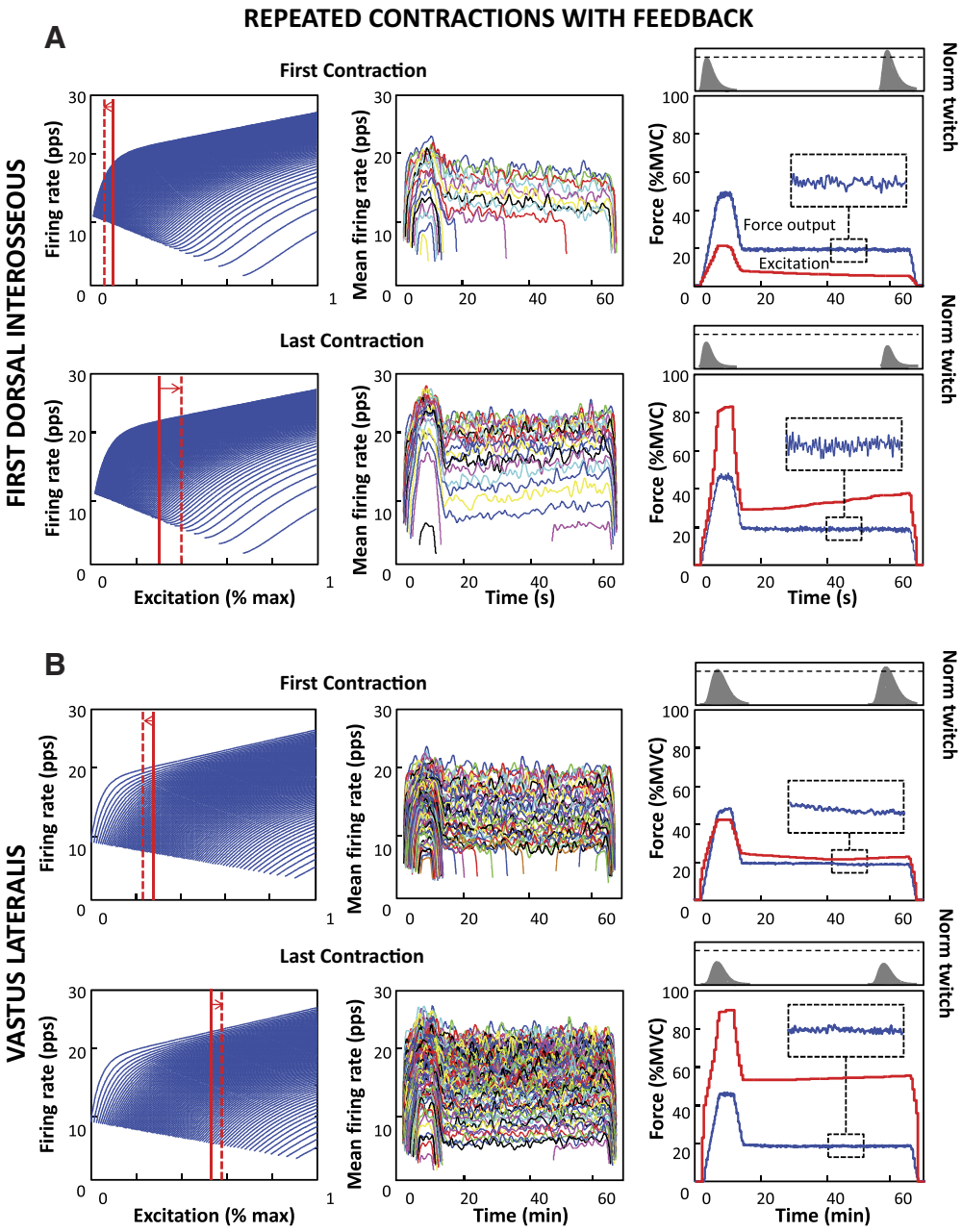

Fig. 7. *A* and *B*: simulated intermittent contraction series for the FDI (*A*) and VL muscles (*B*). The first (*top*) and last contraction of the series before the endurance limit (*bottom*) are presented. The simulation mimics the experimental protocol of Adam and De Luca (2003, 2005). Data are presented in a similar manner as in Fig. 6. Note that the simulation was able to track the force increasing segment of the contraction as well as the constant force segment. During the constant force segment of the first contraction, the excitation to the motoneuron pool decreases due to the increase in muscle force twitch amplitude, causing a decrease in the firing rates of the active motor units and derecruitment of several motor units. The opposite phenomena occur as the contraction is sustained longer. The force remains at the constant target value throughout the simulation and presents a marked increase in force fluctuations.

Figure 8 presents a comparison of the simulated mean firing rate data for the series of repeated intermittent contractions of Fig. 7*B* (*top*) with the empirical data from a similar protocol performed with the VL muscle by Adam and De Luca (2005) (*bottom*). The black line represents the amplitude of the muscle force twitch, and the colored lines are the mean firing rates of a sample of motor units active during the lower 20% MVC plateau region of the force trajectory. In the empirical data, motor unit firing rates were analyzed only in *contractions 1*, *2*, *3*, *5*, *7*, *9*, and *10*, whereas the results from all contractions are presented for the simulated data. Note the remarkable similarity of the two sets of data. In both sets, the muscle force twitch increases after the second contraction and then decreases continuously to the endurance limit on the 10th contraction. The firing rates initially decrease during the first contraction and then continuously increase in subsequent contractions. In the simulated data, the first two motor units, those with the greatest firing rates and presented with the dashed lines, show only a minor increase in their firing rates as the contractions progress. This is so because these two motor units have almost reached their firing plateau at 20% MVC; a fact that is clearly evident in the firing rate spectrum of Fig. 2. In fact, it is plainly obvious that the increase in the firing rates is greater for later-recruited motor units in both the simulated data and the empirical data of Fig. 8.

The simulated data and the empirical data also show two other noteworthy factors. As the firing rate increases during subsequent contractions, new motor units are recruited. This behavior is expected as the operating point of the excitation increases to compensate for the decreasing amplitude of the force twitches.

In a corollary fashion, it can be seen in the simulated data that during the first contraction, where the amplitude of the

Table 2. *Intermittent contraction series*

	Intermittent Contractions			
	FDI		VL	
	First contraction	Last contraction	First contraction	Last contraction
Contraction	1	14	1	10
Excitation at 50% MVC, %max	20.2	87.5	44.4	93.8
Excitation at 20% MVC at onset, %max	8.9	30.6	27.3	56.3
Excitation at 20% MVC at end, %max	5.3	39.6	23.7	58.6
No. of active MUs at 50% MVC	100	120	424	598
No. of active MUs at 20% MVC at onset	62	110	245	498
No. of active MUs at 20% MVC at end	45	115	(208) 224	509
No. of MUs recruited				
0–10% MVC	38	88	152	407
10–20% MVC	22	17	91	68
20–30% MVC	16	9	68	48
30–40% MVC	12	4	56	38
40–50% MVC	12	2	57	37
Average MU firing rate at 20% MVC, pps	14.82 (11.3–18.2)	18.3 (7.4–23.1)	13.7 (7.9–20.6)	16.3 (5.9–23.4)
Force CV at 20% MVC, %	1.4	2.5	0.6	1.0
Normalized twitch at 20% MVC at onset	1	0.67	1	0.65
Normalized twitch at 20% MVC at end	1.21	0.55	1.08	0.60

Data are results of the simulations of the series of repeated intermittent contractions for the FDI and VL muscles. CV, coefficient of variation.

force twitches increase, several higher-threshold motor units, those with the lower firing rates (2 are displayed in Fig. 8*A* in brown and magenta) become derecruited and quickly re-recruited as, apparently, the muscle force twitch stopped potentiating in the middle of the first contraction. The early derecruitment was not seen by Adam and De Luca (2005). That is likely due to the low probability of detecting a derecruited motor unit. According to the simulation, 37 of 245 motor units would derecruit during the first contractions, which represent 15% of all motor units active in the entire muscle. The decomposition technology used by Adam and De Luca (2005) used a highly selective fine-wire sensor that could detect only 3–5 motor units during the 20% MVC plateau region of the first contraction. The probability of detecting one of the derecruited motor units is low. However, the new surface electromyography (sEMG) decomposition technology used in this study did find evidence of the early derecruitment of motor units ~25 s into a recently collected constant-force contraction at 50% MVC in the VL muscle (unpublished data) (see Fig. 9).

With findings similar to the simulated data, Adam and De Luca (2005) also observed one re-recruited motor unit during the 20% MVC plateau region of the first contraction. From this observation, they hypothesized that the peak of the potentiation phase occurred before the end of the first contraction, most likely around 40 s, when the re-recruited motor unit was detected. The actual presence of the potentiation peak at 40 s could not be noticed in the empirical data because the stimulation was only performed in between contractions. We based our time-dependent changes in the muscle force twitch on the results of Adam and De Luca

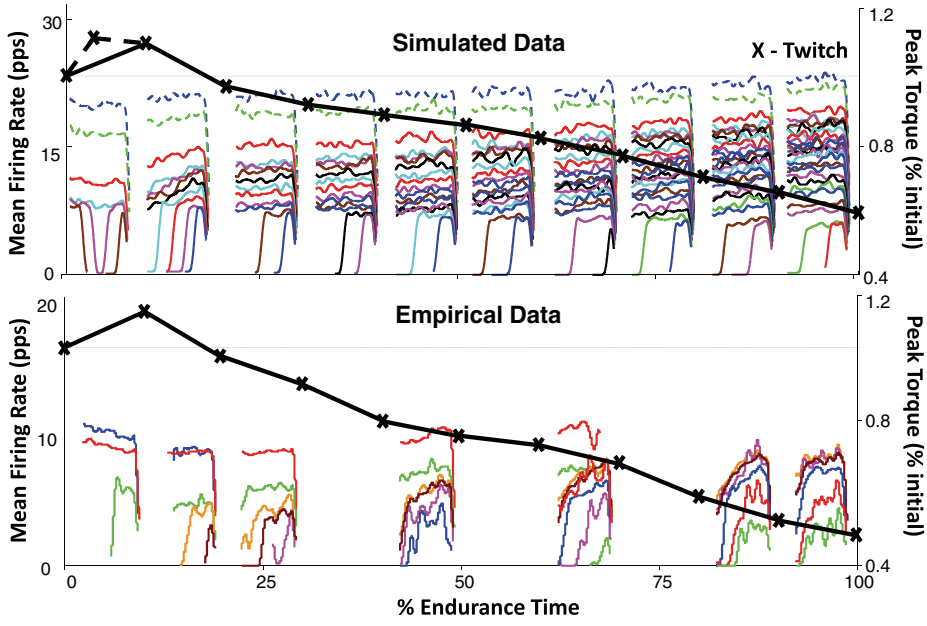

Fig. 8. A comparison between the empirical data (*top*) from Adam and De Luca (2005) and those simulated from the model for an equivalent protocol (*bottom*). Note the similarity. In both cases the firing rates decrease slightly during the first contractions; they subsequently increase up to the endurance limit. Additional later-recruited lower-firing-rate motor units are recruited as time progresses. The thick black lines represent the simulated (*top*) and empirical (*bottom*) modulating amplitude of the whole muscle force twitch, which potentiates slightly during the first contraction and then decreases to the endurance limit. Refer to the text for additional details.

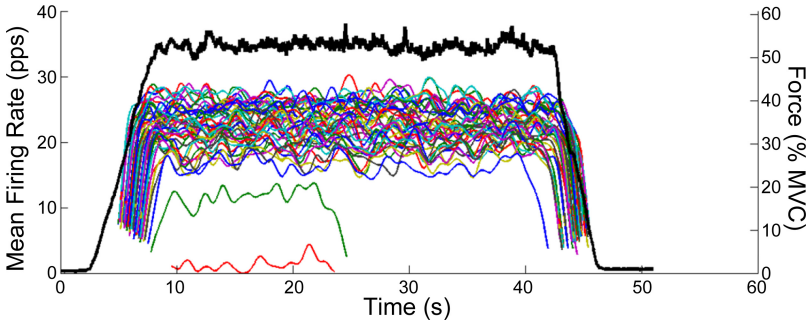

Fig. 9. An example of 2 motor units being derecruited during the early phase of a 50% MVC constant-force isometric contraction from the VL muscle (unpublished data). The colored lines indicate the firing rates of the coactive motor units, and the dark line represents the produced force.

(2003, 2005); thus, in our model, the peak of the muscle force twitch occurs at 40 s, as highlighted by the dotted black line in Fig. 8, *top*.

Repeated intermittent contractions with delayed error correction. Figure 10, *A* and *B*, presents the results of the simulation of the repeated intermittent contractions when the excitation is adjusted every 150 ms for the FDI and VL muscle, respectively, proportionally to the error between the target force and the simulated output force. Data are presented in a similar manner as in Fig. 7.

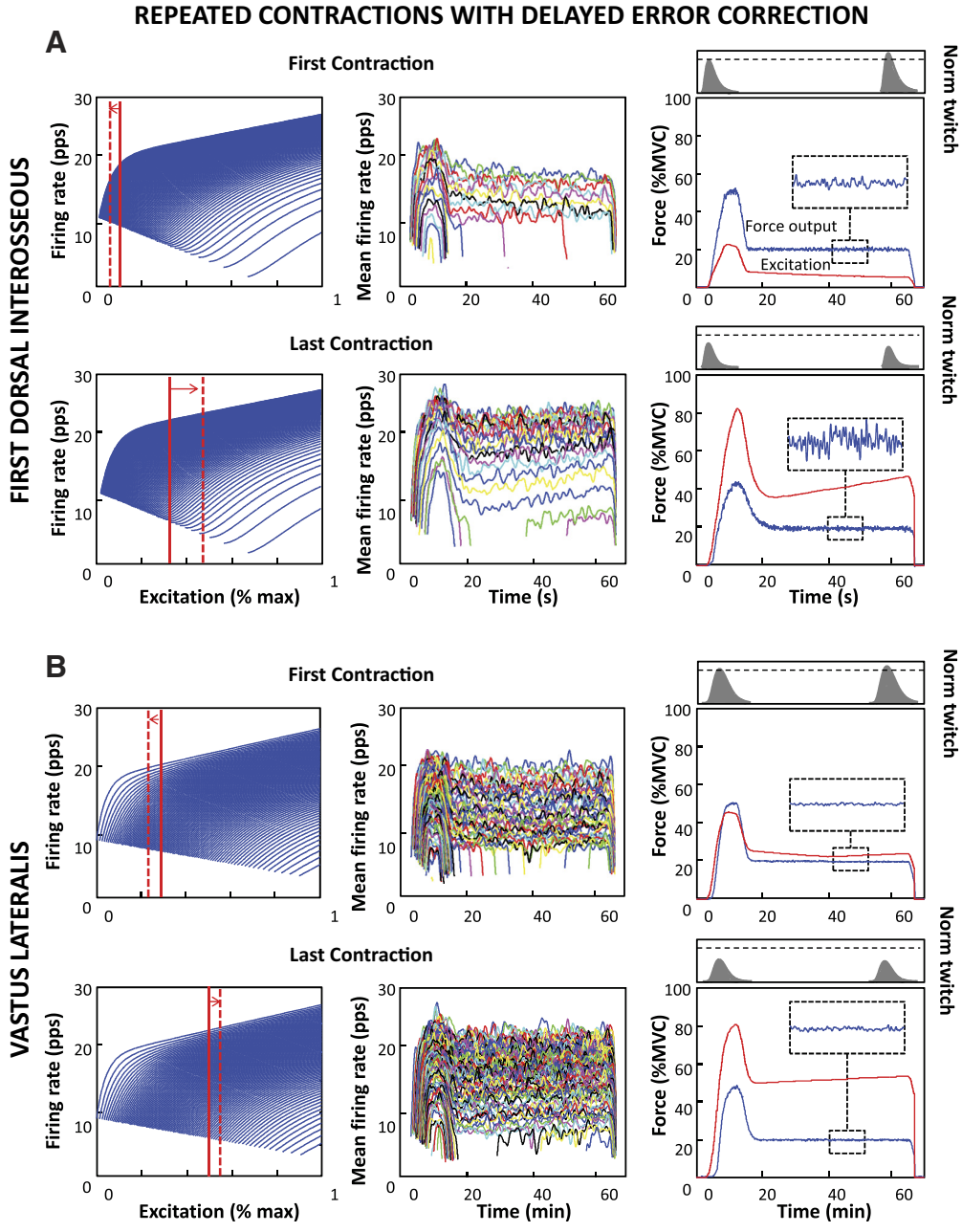

Fig. 10. *A* and *B*: simulated intermittent contraction series for the FDI (*A*) and VL muscles (*B*) with delayed tracking error correction. The first (*top*) and last contraction of the series before the endurance limit (*bottom*) are presented. Data are presented in a similar manner as in Fig. 7. Note that the motor unit behavior and the muscle force behavior show patterns similar to those presented in Fig. 7. Refer to the text for additional details.

As can be noted by comparison with Fig. 7, the motor unit firing behavior and force characteristics obtained with the two different force feedback modalities are similar. During the 20% MVC plateau region of the first contraction, the input excitation decreased slightly in both muscles, leading to decreasing firing rates of the active motor units and derecruitment of several motor units, while the muscle force twitch amplitude increased. Nineteen motor units were recruited again at the end of the plateau phase in the VL muscle, when the muscle force twitch started to decrease. Throughout the series of repeated contractions as the muscle force twitch amplitude decreased, the input excitation needed to exert both the initial 50% MVC and subsequent 20% MVC force increased progressively with contraction time, leading to a progressively greater number of recruited motor units and increasing firing rates. These adjustments are presented in Fig. 10 and Table 3 for the first and last contraction of the series in both muscles. The coefficient of variation of the force increased with contraction time.

DISCUSSION

The model described in this article supports the notion that the force output of a muscle is regulated by a modulation of the common drive to the motoneuron pool, which represents the net excitation provided by the CNS and the PNS, in response to modulations of the force twitches of the motor units to produce a given muscle force output. As the muscle mechanical response varies, the input excitation is required to change to maintain a target level of muscle force output, leading to the expected modifications in motor unit firing rates. The essential result of this model is that this simple feedback scheme reproduces the firing rate and force behavior observed in empirical data from our previous experiments (Adam and De Luca 2003, 2005), as well as those of other investigators (Bigland-Ritchie et al. 1986; De Ruiter et al. 2004; Dorfman et al. 1990; Person and Kudina 1972; Shimizu 1990; among others). Thus it appears that the force twitch characteristics are a dominant causal factor determining the firing rate behavior and the characteristics of the output muscle force; a hypothesis first proposed by De Luca (1979) and later by De Luca et al. (1996).

The model is not intended to replicate all the electrochemical and mechanical processes involved in muscle force production. Instead, it is based on mathematical descriptions of the motor unit firing rate behavior and force twitches derived from empirical data.

Caveats of the model. The relation between the input excitation and the firing rates of the motoneurons is described by a "firing rate spectrum" developed by De Luca and Contessa (2012). In the present construction of the model, the firing rate spectrum is maintained invariant with contraction time, because the requisite information is not available. However, when it becomes available, the information of any time- or activation-dependent changes in the excitation-firing rate relation or in the intrinsic firing properties of motor units (Powers et al. 2011) may be included in future evolutions of the firing rate spectrum. Even with this present limitation, it seems that the time dependence of the firing rate spectrum is not likely to have a dominant role in shaping the production of the force output over the time course of the sustained fatiguing contractions simulated here, because the model produces force and firing rate behavior that compares well with reported empirical data.

The force feedback implemented to regulate the input excitation is intended to maintain the force output at a required target level, such as when the muscle force diverges from the target force during visual tracking tasks. The simulated motor unit firing rate and force behavior is qualitatively similar when the feedback occurs with no time delay or 150-ms time delay, as would be the case with visual feedback (Slifkin et al. 2000). We have used the example of visual feedback to show that adding a delay to the feedback does not alter the characteristics of the simulated firing rate behavior. Compare the results of the

Table 3. *Intermittent contraction series with delayed tracking error correction*

	Intermittent Contractions–Delayed Feedback			
	FDI		VL	
	First contraction	Last contraction	First contraction	Last contraction
Contraction	1	14	1	10
Excitation at 50% MVC, %max	22.4	82.0	45.7	80.9
Excitation at 20% MVC at onset, %max	9.4	35.9	29.7	49.6
Excitation at 20% MVC at end, %max	5.4	46.9	23.9	53.5
No. of active MUs at 50% MVC	102	120	433	579
No. of active MUs at 20% MVC at onset	65	113	344	460
No. of active MUs at 20% MVC at end	45	117	(208) 227	483
No. of MUs recruited				
0–10% MVC	31	33	19	19
10–20% MVC	29	45	76	79
20–30% MVC	17	27	149	187
30–40% MVC	12	9	104	173
40–50% MVC	13	6	85	121
Average MU firing rate at 20% MVC, pps	15.0 (11.5–18.0)	19.1 (8.2–23.7)	13.8 (8.2–20.8)	16.5 (7.6–23.1)
Force CV at 20% MVC, %	1.9	2.4	0.6	0.8
Normalized twitch at 20% MVC at onset	1	0.64	1	0.7
Normalized twitch at 20% MVC at end	1.21	0.52	1.08	0.7

Data are results of the simulations of the series of repeated intermittent contractions for the FDI and VL muscles with delayed tracking error correction.

simulation where feedback is not delayed in Fig. 7 with those of the delayed feedback simulation of Fig. 10. By using the visual time delay we do not mean to imply that only the visual system can provide a delay in the feedback. Surely, other sensors such as the Golgi tendon organs, joint receptors, skin receptors, and spindles could provide feedback information that is related to the divergence of the force output from a target force. However, regardless of the feedback and the sensors used to detect the force output, the error adjusts the excitation to the motoneuron pool to perform the required tracking task.

In this work we focused on contractions where muscle force is maintained at a constant level over time. As mentioned earlier, the same force regulation concept is likely to explain the regulation of varying muscle force. This later point is made clear by the force paradigm modeled in Fig. 7, where the force output initially increases to 50% MVC and later decreases to 20% MVC. Motor units are recruited and increase their firing rates as the net input excitation increases to produce a 50% MVC output force. Therefore, it appears that the force output of a muscle is regulated in the same manner whether it remains constant over time or varies in amplitude.

In the simulation of sustained submaximal contractions with force feedback, the net excitation to the motoneuron pool increases to maximal levels, at which point the endurance limit is reached. However, in real experimental conditions, contractions might terminate prematurely before the excitation reaches maximal levels if subjects experience discomfort and pain or if they are not well trained or motivated, all factors that are not considered in this model. Also note that the simulated input excitation represents the net excitation to the motoneuron pool, and thus it consists of the summed effect of central and peripheral inputs. In doing so, our approach does not require us to model separately the contributions to the net excitation from the CNS and the PNS, respectively.

Firing rate behavior during force-varying or sustained contractions. In the simulations of both the sustained and intermittent contractions, the firing rates of all active motor units first decrease for about 60 s or less and subsequently increase, following the behavior of the excitation, which responds to the time-dependent modulation of the force-twitch amplitude. (See the mean firing rate trajectories in Figs. 6, 7, and 10, *middle* panels.) These results are consistent with the findings of our previous work (Adam and De Luca 2005; De Luca 1979; De Luca et al. 1982b, 1996) and are supported also by the results of Person and Kudina (1972), Bigland-Ritchie et al. (1986), Shimizu (1990), Dorfman et al. (1990), and De Ruiter et al. (2004).

In contrast, studies by Christova and Kossev (2001) and Kuchinad et al. (2004) report a continuous decrease in firing rates during submaximal contractions. In Christova and Kossev (2001), the difference is likely due to the analysis of grouped data averaged among different motor units and different subjects. Pooling data confuses the structure of the firing rate behavior, especially during fatiguing contractions, where the firing pattern varies over time and among subjects. In the work of Kuchinad et al. (2004), the authors reported an increased contribution of the agonist muscles to the total torque, which raises concerns over the force generated by the monitored muscle. In all the cited studies, what is commonly designated as force is actually the torque generated by the active muscle around the joint being monitored. Keeping the torque constant does not guarantee that the individual force of the monitored muscle remains constant. It was for precisely this reason that Adam and De Luca (2005) monitored the surface EMG signals of the synergist and antagonist muscles while performing the repeated-contraction paradigm. They analyzed only the data collected from experiments where the relative amplitude of the EMG signals from the agonist and antagonist muscles remained constant, indicating that the relative force contribution of each muscle remained constant with respect to the measured torque around the joint. Garland et al. (1994, 1997) described decreased firing rates for earlier-recruited motor units, whereas later-recruited motor units increased their firing rates. However, they generally observed the firing pattern of earlier-recruited motor units during the first part of the fatigue protocol and that of later-recruited motor units near the endurance limit. Hence, their observations do not provide a complete or continuous expression of motor unit behavior and suggest that the firing patterns would support our findings if they were to be followed for the entire duration of the fatiguing protocol. Carpentier et al. (2001) reported a steady decrease in the firing rates of earlier-recruited motor units, whereas later-recruited motor units first increased and subsequently decreased their firing rates.

Various suppositions and conjectures have been used to explain these contrasting behaviors. Christova and Kossev (2001) suggested that the CNS modulates the gain of reflex pathways, leading to firing rate decrease of the active motor units, whereas the common central drive increases, causing recruitment of new motor units. The two phenomena hypothetically "optimize" the activity of individual motor units that are in different functional states during prolonged contractions. Similarly, Garland et al. (1994, 1997) suggested that some mechanisms, such as motoneuron adaptation or afferent feedback, prevent the increased excitatory drive from increasing the firing rates of the active motoneurons and that newly recruited motor units are less affected by this influence and thus increase their firing rates. Along the same line, Carpentier et al. (2001) hypothesized that different motor unit firing adaptations are the consequence of variable contributions from motoneuron adaptation and afferent feedback. Some of the above-mentioned mechanisms, such as motoneuron adaptation, increased reflex inhibition, or spindle afferent input, might develop during sustained or repeated contractions. However, it is difficult to imagine individual diversified feedback to the motor units in the motoneuron pool, since afferent feedback has an approximately uniform synaptic input to the motoneuron pool (Lüscher et al. 1979; Mendell and Henneman 1968). Even if the above-mentioned physiological phenomena do occur, the model indicates that the varying characteristics of the force twitches alone explain the motor unit firing rate behavior reported during sustained isometric contractions by Adam and De Luca (2005).

"Reserve capacity" of muscle. Christova and Kossev (2001) and Kuchinad et al. (2004) proposed that the firing rate decrease observed with fatigue is consistent with the "muscle wisdom" hypothesis advanced by Bellemare et al. (1983), Bigland-Ritchie et al. (1983), and Marsden et al. (1983) from the analysis of sustained MVCs. This hypothesis stipulates that the drive to the motoneuron pool adapts to match the slowing of the muscle fiber contractile properties during fatigue and

that it "optimizes" force production while preventing contractile failure. In this way, as contractile speed slows, firing rate declines accordingly, since a higher firing rate would not provide additional force (Bigland-Ritchie et al. 1983). From this perspective, the muscle wisdom hypothesis does not leave any force reserve in the muscle, unless it is hypothesized that there exist a "reserved" group of motor units that would lie in wait of the rare circumstances when they might be needed. However, such dormancy raises the question as to why they would not atrophy from lack of use, as all other muscle fibers do when not activated for a long time.

Our model contains no set-aside group of motor units. However, the higher-threshold motor units fire at the lowest firing rates during normal voluntary contractions. Thus they have the capacity to fire faster, as they do when electrically stimulated as shown by Eccles et al. (1958) and Kernell (1965b). Consequently, supramaximal forces could be produced in stressful circumstances due to hyperactivation of the high-threshold motor units, as previously suggested by De Luca et al. (1982a), De Luca (1995), and Erim et al. (1996), which may be triggered possibly by some stress-related mechanism or some other triggering mechanism. As may be seen in Figs. 3 and 4, the higher-threshold motor units have force twitches that are orders of magnitude greater than those of the very-low-threshold motor units and are capable of generating a great amount of force.

Motor unit recruitment and derecruitment behavior during force-varying or sustained contractions. Three observations were made throughout the course of the simulated force contractions to the endurance limit. The first is that some motor units are derecruited as force twitches increase (potentiation) and the firing rates of the active motor units decrease. Verification of this prediction has been elusive, most likely due to technical difficulties. However, we have recently been able to detect derecruitment at the beginning of a constant-force contraction using the sEMG decomposition technology described by De Luca et al. (2006) and Nawab et al. (2010). An example is depicted in Fig. 9 and is discussed in RESULTS.

The second observation is that additional motor units are progressively recruited as the contraction is sustained for longer periods of time, the amplitude of the motor unit force twitches diminishes, and the firing rates of the active motor units increase. The recruitment of new motor units throughout the duration of the contraction has been observed in several studies (Adam and De Luca 2003; Bigland-Ritchie et al. 1986; Broman et al. 1985; Carpentier et al. 2001; De Luca et al. 1996, 2008; Dorfman et al. 1990; Garland et al. 1994, 1997; Thomas and Del Valle 2001). The increase in the firing rates and the recruitment of new motor units predicted by the model are consistent with the often noted increase in the amplitude of surface EMG signal that occurs during sustained fatiguing contractions (Adam and De Luca 2005; Basmajian and De Luca 1985; De Ruiter et al. 2004).

The third observation is that motor units are recruited at lower force thresholds as the muscle fatigues during the sequence of sustained contractions, as shown in Tables 2 and 3. Note the number of motor units activated at each recruitment interval from 0 to 50% MVC in the last contraction of the series with respect to the first contraction of the series. This prediction by the models is supported by the work of Adam and De Luca (2003), Garland et al. (1994), and Maton and Gamet (1989).

Our model indicates that recruitment and derecruitment behavior can be related to changes in the motor unit force twitch and force-generating capacity. Thus time-dependent changes in the mechanical aspects of the motor units should always be taken into consideration in the analysis of the activation and deactivation behavior of motor units. For instance, a decreased recruitment threshold in repeated contractions has been considered as potential proof for the existence of persistent inward currents (PICs) in human subjects (Gorassini et al. 2002a, 2002b). Although PICs might actually develop in human subjects performing voluntary contractions, our simulated results indicate that such interpretation needs to be made with caution, because the time-dependent changes in the motor unit force twitches during a contraction can also cause recruitment/derecruitment alterations.

Force fluctuation during force-varying or sustained contractions. The simulation results of the sustained and repeated intermittent contractions with force feedback produced a force that displayed progressively increasing variability. As an example, compare the *top* and *bottom right* panels of Figs. 6, 7, and 10 in both the FDI and VL muscles. This observation has been consistently reported in studies of fatiguing constant-force contractions (Contessa et al. 2009; Furness et al. 1977; among others). We also noted that in the simulation with no force feedback, the force variation remained constant throughout the contraction. In that simulation, no motor units were recruited throughout the contraction, as the excitation was maintained constant. This finding indicates that the force fluctuation increases as higher-threshold motor units are recruited throughout the contraction. The latter recruited motor units have force twitches with greater amplitude and shorter time duration; they fire slower and do not tetanize as the lower-threshold faster-firing motor units. For clarification refer to Fig. 3*E*, where the forces generated by five motor units (*motor units 1*, *30*, *60*, *90*, and *120*) in the FDI muscle are displayed.

Yao et al. (2000) and Moritz et al. (2005) have suggested a causal relation between increase in force variability and increase in motor unit synchronization and firing rate variability. In contrast, our recent work (Contessa et al. 2009) showed no evidence of increased synchronization and firing rate variability during sets of repeated contractions to the endurance limit. Our model did not include synchronization between motor unit firings, and the firing rate variability was maintained at a constant value throughout the simulations. It is apparent that the increased variation of muscle force during sustained contractions is not dominantly induced by changes in the firing properties of motoneurons and may result purely as a response to the mechanical property of newly recruited motor units.

The simulations of the FDI muscle showed greater force variability than those of the VL muscle. This observation may be explained by *1*) the presence of a greater number of motor units in the VL muscle, which, unlike the FDI, are recruited throughout almost the entire excitation spectrum (De Luca and Hostage 2010; De Luca and Kline 2012); and *2*) the more similar shape and longer time duration of the motor unit force twitches in the VL muscle, which, unlike the FDI, favor tetanization and smoother force production. For clarification see Figs. 6 and 7.

The degree of force variability predicted by the model in the VL muscle is consistent with that found by Contessa et al. (2009) in empirical data from a similar protocol of repeated intermittent contractions. In that study the coefficient of variation of the force increased from an average value of 0.7 $\pm$ 0.2% in the first contraction to an average value of 2.1 $\pm$ 1%

in the last contraction at the endurance limit. The same protocol performed on the FDI muscle of 7 subjects showed an increase in the coefficient of variation of the force from 1 ± 0.5% to 3 ± 1% (unpublished observations).

In summary, the force feedback model explains the firing rate and recruitment/derecruitment behavior of motor units that have been described in several published studies, including that of our own sustained constant-force contractions. The model was able to predict the derecruitment of motor units and the firing rate decrease at the beginning stage of a sustained contraction and the subsequent recruitment of motor units as the contraction continued. In both force-increasing and constant-force contractions, the firing rate and the recruitment characteristic were symbiotically modulated as the operating point of the excitation to the motoneuron pool responded to the error that measured the difference between the target force and the produced force.

The model explains the pattern of the varying force fluctuation that occurs during sustained contractions. It points to the recruitment of increasing larger motor units as the cause. It cautions the use of motor unit behavior at recruitment and derecruitment as an indication of PICs. It provides an alternative mechanism for the reserve capacity of motor units to generate extraordinary force. Finally, *1*) the model supports the hypothesis that the control of motoneurons remains invariant during force-varying and constant-force isometric contractions, and 2) although other factors may be involved, the model indicates that the mechanical characteristics of the force twitch alone might explain much of the experimental observations of motor unit control reported in the literature.

APPENDIX A: THE FIRING RATE SPECTRUM

We have shown in previous studies (De Luca and Contessa 2012; De Luca and Hostage 2010) that the range of firing rates of all motor units is bounded when the excitation progresses from zero to maximal level and that this range is muscle dependent. When the muscle force increases linearly, the firing rate trajectories may be suitably approximated with an exponential function whose time constant progressively increases for motor units with increasing recruitment threshold. A complete description of the mean firing rate behavior of a specific motor unit i recruited at the threshold force τ_i, increasing over time as the force φ of the contraction varies, is given by the following equation, whose parameters can be customized to a specific muscle (for details see De Luca and Contessa 2012):

$$\lambda_i(t, \varphi, \tau_i) = E + D\varphi + (C - A^{-\frac{\varphi}{B}})\tau_i - e^{\frac{(\mathrm{tr}_i - t)}{m_\theta \tau_i + b_\theta}} \times [E - b_\mathrm{r} + D\varphi + (C - m_\mathrm{r} - Ae^{-\frac{\varphi}{B}})\tau_i] \quad (10)$$

for $t \geq \mathrm{tr}_i$, $0 < \tau_i < 1$, and $\tau_{i+1} > \tau_i$, where tr_i is recruitment time. For a description of the parameters used, refer to De Luca and Hostage (2010) and De Luca and Contessa (2012) where these equations were derived. The values reported for the parameters *A, B, C, D, E,* m_θ, and b_θ are 85, 0.32, −23, 6.93, 20.9, 1.86, and 0.51 for the FDI muscle and 116, 0.15, −21, 8.03, 19.0, 1.59, and 0.38 for the VL muscle (De Luca and Contessa 2012; De Luca and Hostage 2010).

This equation was derived during isometric contractions where the force varies linearly with time, and it can be expressed as a function of force or, equivalently, of the excitation required to achieve a given percentage of maximal force level:

$$\lambda_i(t, \varphi, \tau_i) = E + D\varphi + (C - A^{-\frac{\varphi}{B}})\tau_i - e^{\frac{(\tau_i - \varphi)}{(m_\theta \tau_i + b_\theta) d\varphi/dt}} \times [E - b_\mathrm{r} + D\varphi + (C - m_\mathrm{r} - Ae^{-\frac{\varphi}{B}})\tau_i], \quad (11)$$

where $d\varphi/dt$ is the rate of force increase, which is equal to 10% MVC/s in the simulations presented in RESULTS and in De Luca and Contessa (2012). *Equation 11* customized for the FDI and VL muscle is reported in *Eqs. 1* and *2*, respectively.

This general equation describes the family of firing rates of the motor units in a muscle during an isometric contraction as the force increases from 0 to maximal level (MVC). The firing rate spectrum (*top*) and the histograms of the recruitment threshold distribution (*bottom*) are reported in Fig. 2 for both the FDI and VL muscles. As mentioned in METHODS, a specific level of net excitation is represented as a vertical line set at a specific excitation level (here set at 40% of the maximal excitation) and traverses the values of the mean firing rates of all the recruited motor units located to the left of the spectrum (identified as blue in Fig. 2). If the excitation varies over time, the vertical line will move in the plane. Specifically, it will move to the right in the event of an increase in the net input excitation, leading to recruitment of additional motor units and increase in the firing rates of the active motor units. We have shown that this simulation procedure explains the empirical data reported by Adam and De Luca (2005) during sustained isometric contractions and does not require time-dependent modifications to the firing rate spectrum describing the relation between net input excitation and motor unit firing rates.

APPENDIX B: IMPULSE TRAIN GENERATOR

Impulse train generator. The average firing rate value of each motor unit in the firing rate spectrum is transformed into an impulse train by using the integral pulse frequency modulation method, which produces a spike train with a frequency equal to the numerical value of the average firing rate input. This process consists of integrating the signal input over time and generating an impulse every time the threshold value 1 is reached. At this point, the integrator resets back to 0 and the process begins again.

Noise in the impulse train. The IPI between two adjacent firings of a motor unit can be regarded as a bounded random variable described by a Gaussian distribution and a constant coefficient of variation (CV) ranging between 10% and 30% for all motor units (Clamann 1969; Macefield et al. 2000; Moritz et al. 2005; Nordstrom et al. 1992). Other studies have reported that the IPIs of motor units have a skewed distribution (De Luca and Forrest 1973; Person and Kudina 1972). However, a Gaussian distribution is used here for the sake of simplification. For each motor unit i in the pool, IPIs are generated from a normal distribution with a mean equal to the average IPI of the impulse train and coefficient of variation equal to 20%. Noise is introduced by adjusting the firing instance of each pulse in the train following the equation (Fuglevand et al. 1993):

$$t_{i,j} = t_{i,j-1} + \mu + \sigma Z, \quad (12)$$

where $t_{i,j}$ is the time of the jth firing instance of motor unit i, $t_{i,j-1}$ is the time occurrence of the preceding firing, μ is the mean firing rate of the impulse train, σ is the standard deviation of the IPIs ($\sigma = \mathrm{CV}\mu = 0.2\mu$), and the Z score represents how far a generated value of IPI deviates from the mean of the distribution. Z scores are randomly picked from the interval [−3.9, 3.9], allowing the instantaneous IPIs to deviate less than four standard deviations from the mean of the distribution.

APPENDIX C: MOTOR UNIT FORCE TWITCHES

For the FDI muscle, values for the twitch parameters are available from the literature. The range of peak tension values, P, is quite broad (130-fold), the distribution is skewed toward a greater number of low-force-amplitude motor units, and a positive correlation is reported between recruitment threshold and twitch tension (Elek and Dengler 1995; Gossen et al. 2003; Milner Brown et al. 1973; Stephens and Usherwood 1977; Thomas et al. 1986). Thus we modeled the peak tension P_i as a

Table A1. *Parameters for modeling the force twitches in the FDI muscle*

Reference	Peak Force, mN	Rise Time, ms	Half-Relaxation Time, ms	Duration, ms	Method
Young and Meyer (1981)	35 ± 48	65 ± 18			IMS
	2.14–430	34–140			
Elek et al. (1992)	16 ± 18.7	63 ± 15	61 ± 17		IMS
	1–137	30–110	20–105		
	10.3	62	58		
Kossev et al. (1994)	14.9 ± 16.3	63.1 ± 14.7	60.4 ± 16.4		IMS
	1–140	30–135	24–130		
	9.6	61.7	57.5		
Elek and Dengler (1995)	14 ± 15	64 ± 14	61 ± 16		IMS
	1–140	30–130	20–130		
	9	63	59		
McNulty et al. (2000)	14.7	70.3 ± 5.0	70.2 ± 6.5		INS
	2.2–72.8	32–111.3	20–115.9	101.3–468.8	
	14.7			183.8	

Values for the parameters of the force twitch of the FDI muscle were obtained from the literature. These were used to model the distribution of the peak twitch amplitude, rise time, and half-relaxation time. IMS, intramuscular stimulation; INS, intraneural stimulation.

linear function of motor unit recruitment threshold, with $P_1 = 1$ and $P_n = RP$, where RP = 130 is the range of peak twitch forces and n is the number of motor units in the muscle; $n = 120$ for the FDI (Feinstein et al. 1955) and $n = 600$ for the VL (Christensen 1959). The rise time, Tr, and the half-relaxation time, Thr, display a unimodal distribution: faster-twitch motor units have large twitch tensions, although there are also many motor units with small twitch tensions and fast rise times (Elek and Dengler 1995; Gossen et al. 2003; Young and Meyer 1981). Tr varies over a smaller range compared with peak forces (4-fold) and presents values between 30 and 125 ms, with a mean ± SD of 65 ± 13 ms. In the model, values of Tr for all the motor units in the pool are generated from a Weibull distribution with a mean equal to 65 ms and SD equal to 13 ms. The parameters of the Weibull distribution that match these values are $k = 39.23$, $\beta = 2.93$, and $\alpha = 30$. Thr has a slightly broader range (5.5-fold, range 20–120), with a mean equal to 63 and SD equal to 14 ms. Similarly to Tr, values for Thr are generated from a Weibull distribution with the reported mean and SD. The parameters that match these values are $k = 47.87$, $\beta = 3.39$, and $\alpha = 20$. Table A1 reports the data used to estimate the values of the parameters for the FDI muscle.

For the VL muscle, no force twitch data are available from the literature. Thus we based our estimate on previous data obtained in our laboratory. Adam and De Luca (2003, 2005) electrically stimulated the VL at supramaximal intensity to obtain the whole muscle force twitch. The average peak value was 46 N, the average Tr was 135 ms, and the average Thr was 79 ms. We assumed that similar distributions of force twitch parameters apply to both the VL and the FDI muscles: P was described as a linear function of recruitment threshold; Tr and Thr were generated from a Weibull distribution. The range of peak forces RP was set to 150, a value derived from the tibialis anterior muscle (Feiereisen et al. 1997). Values for the Weibull distribution defining Tr and Thr were varied to generate different distributions of force twitches. The individual twitches were summed to obtain the whole muscle twitch, and the distribution that resulted in the whole muscle twitch closest to that which was experimentally observed was chosen. The resulting parameters of the Weibull distribution were $k = 115$, $\beta = 4.5$, and $\alpha = 50$ for Tr and $k = 70$, $\beta = 4.5$, and $\alpha = 15$ for Thr. We appreciate that this approach for obtaining the parameter values only provides estimates; nonetheless, it is a reasonable approximation. As experimental data on the ranges and values of the force

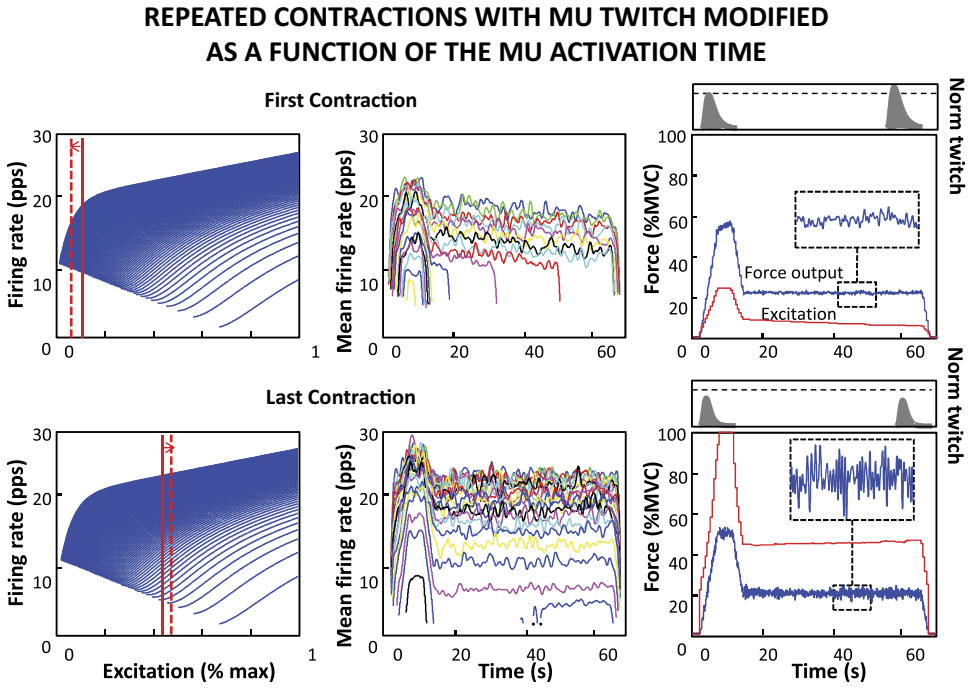

Fig. A1. Simulated intermittent contraction series for the FDI muscle with the pattern of time-dependent change in the amplitude of the force twitches applied to all active motor units as a function of their individual activation time instead of the contraction time (as in Fig. 7). The first (*top*) and last contraction of the series before the endurance limit (*bottom*) are presented. Data are presented in a similar manner as in Fig. 7. Note that the motor unit behavior and the muscle force behavior show patterns similar to those presented in Fig. 7. Refer to the text for additional details.

Table A2. *Nonuniform behavior of the force twitches*

	FDI: Intermittent Contractions	
	First contraction	Last contraction
Contraction	1	34
Excitation at 50% MVC, %max	22.1	100
Excitation at 20% MVC at onset, %max	9.2	43.7
Excitation at 20% MVC at end, %max	5.2	46.4
No. of active MUs at 50% MVC	102	120
No. of active MUs at 20% MVC at onset	61	116
No. of active MUs at 20% MVC at end	45	117
No. of MUs recruited		
0–10% MVC	40	108
10–20% MVC	23	7
20–30% MVC	15	3
30–40% MVC	12	1
40–50% MVC	12	1
Average MU firing rate at 20% MVC, pps	14.88 (11.4–18.0)	19.2 (5.5–24.0)
Force CV at 20% MVC, %	1.4	5.6
Normalized twitch P at 20% MVC at onset	1	0.81
Normalized twitch P at 20% MVC at end	1.21	0.76

Data are results of the simulations of the series of the intermittent contraction series with nonuniform force twitch time-dependent behavior. P, peak force.

parameters for the VL muscle become available, the distribution can be adjusted to reflect improved estimates.

The force twitches modeled for the FDI and VL muscles are presented in Fig. 4*A*. The distributions of parameters for both muscles are reported in Fig. 4*B*.

APPENDIX D: TIME DEPENDENCE OF THE MOTOR UNIT FORCE TWITCHES

Information available in the literature on time-dependent changes in the force twitches of individual motor units during a voluntary sustained contraction is scarce. Kernell et al. (1975) reported that potentiation (increase in force twitch amplitude) is more pronounced for higher-threshold motor units; Burke (1967) observed similar increase in the force twitch amplitude irrespective of recruitment threshold; Thomas et al. (1990) reported that low-threshold motor units show the greatest increase in amplitude. Thomas et al. (1990, 1991a) and Fuglevand et al. (1999) reported a linear relation between the amplitude of the force twitch and the motor unit "fatigue index," measured as the peak twitch force after a standard fatigue protocol normalized to the initial nonfatigued value. However, in these studies, all motor units were stimulated at

Table A3. *Time-varying duration of the force twitches*

	FDI: Intermittent Contractions			
	Decreasing twitch duration		Increasing twitch duration	
	First contraction	Last contraction	First contraction	Last contraction
Contraction	1	12	1	16
Excitation at 50% MVC, %max	21.9	65.7	21.5	78.3
Excitation at 20% MVC at onset, %max	9.0	24.0	8.1	28.2
Excitation at 20% MVC at end, %max	5.3	29.8	5.0	33.9
No. of active MUs at 50% MVC	101	119	101	120
No. of active MUs at 20% MVC at onset	62	104	61	108
No. of active MUs at 20% MVC at end	46	110	43	112
No. of MUs recruited				
0–10% MVC	41	77	41	88
10–20% MVC	22	21	22	15
20–30% MVC	14	11	15	9
30–40% MVC	12	7	12	5
40–50% MVC	12	3	11	3
Average MU firing rate at 20% MVC, pps	14.9 (11.3–18.2)	17.4 (8.1–22.3)	14.9 (11.5–17.9)	17.8 (7.4–22.8)
Force CV at 20% MVC, %	1.6	2.1	1.5	2.3
Normalized twitch P at 20% MVC at onset	1	0.79	1	0.64
Normalized twitch P at 20% MVC at end	1.21	0.67	1.20	0.54
Twitch Tr at 20% MVC at onset, ms	50	46	50	49
Twitch Tr at 20% MVC at end, ms	52	45	53	48
Twitch Thr at 20% MVC at onset, ms	100	85	100	95
Twitch Thr at 20% MVC at end, ms	105	82	108	94

Data are results of the simulations of the series of repeated intermittent contractions for the FDI muscle when the duration of the motor unit force twitches varies with contraction time. Thr, half-relaxation time; Tr, rise time.

a fixed frequency of 40 Hz, whereas it is known that during voluntary contractions, higher-threshold motor units fire at progressively lower firing rates (De Luca and Contessa 2012; De Luca and Hostage 2010).

The time-dependent adjustments in the duration of the motor unit force twitches (Tr and Thr) are also not well understood. Carpentier et al. (2001) reported that after fatigue caused by repeated submaximal contractions in the FDI muscle, the average values of P, Tr, and Thr increased for low-threshold motor units and decreased for high-threshold motor units. Thomas et al. (1991a) reported that in response to a standard 2-min fatigue test in the FDI, Tr became slower but Thr became faster for motor units that lost force (lower P), whereas motor units that potentiated (higher P) showed the opposite adaptation. Again, the effect of electrical stimulation on motor unit force twitch is likely to be different than the effect of voluntarily induced muscle fatigue. Overall, these data do not provide a reliable basis for modeling the adjustments in the force twitch parameters for the individual motor units of the FDI muscle. For the VL muscle, to our knowledge no data are available regarding the mechanical properties of individual motor units.

The majority of the studies available in the literature relate to the time-dependent adjustments of the whole muscle force twitch rather than those of the individual motor units. There is general agreement that the amplitude of the muscle force-twitch increases at the beginning of a sustained contraction (potentiation) and subsequently decreases as fatigue progresses (Burke 1981; Dolmage and Cafarelli 1991; Macintosh et al. 1994; Vandervoort et al. 1983). Again, contrasting observations have been reported for the time-dependent parameters of the muscle force twitch with fatiguing contractions: the force twitch became slower in the work of Bigland-Ritchie et al. (1983), faster in Vøllestad et al. (1997), and did not vary in Binder-MacLeod and MacDermond (1993). Some of the variability in the observations might be associated with differences in the fatiguing protocols employed. In our previous work (Adam and De Luca 2003, 2005), the VL muscle was electrically stimulated at supramaximal intensity in the rest periods between a series of repeated isometric

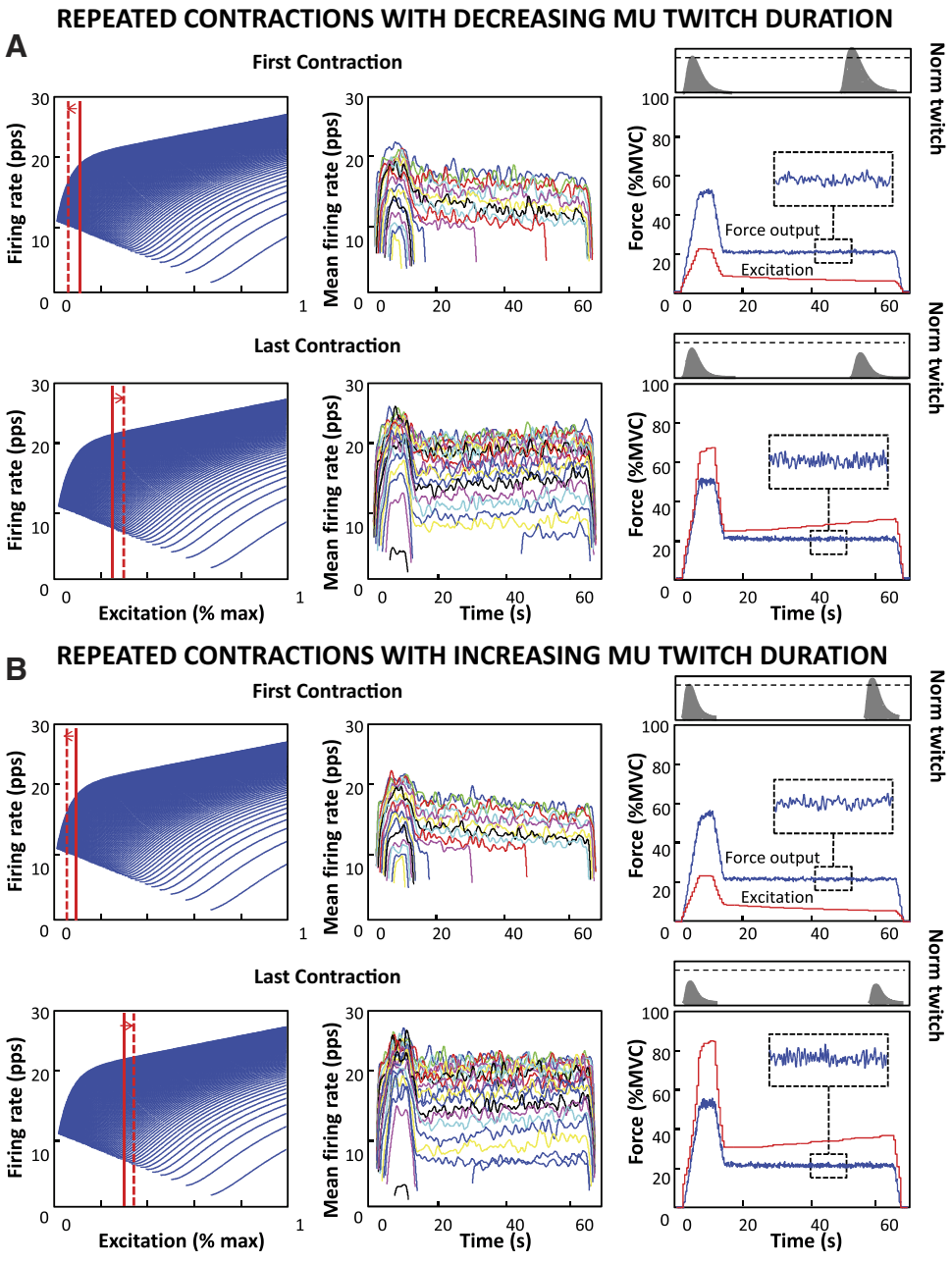

Fig. A2. Simulated intermittent contraction series for the FDI muscle as the motor unit twitch duration shortens (*A*) and lengthens (*B*) with contraction time. The first (*top*) and last contraction of the series before the endurance limit (*bottom*) are presented. Data are presented in a similar manner as in Fig. 7. Note that the motor unit behavior and the muscle force behavior show patterns qualitatively similar to those presented in Fig. 7. Refer to the text for additional details.

contractions sustained at 50% and 20% MVC. Results showed that the muscle force twitch amplitude increased to ~1.1 of the initial value in the first 40 s and decreased to 0.6 of the initial value as the contraction was repeated to the endurance limit (reached after 10 min). There was a tendency for both the rise time and the half-relaxation time to decrease with fatigue, but the change was not consistent in all subjects. When we applied the same protocol to the FDI muscle of seven subjects (unpublished data), the amplitude increased on average to about 1.2 of the initial value in the first 60 s and then decreased to 0.4 of the initial value at endurance time (after about 14 min). Rise time and half-relaxation time declined on average to ~85% and 95% of the initial value, but the trend was not consistent in all subjects. As shown in METHODS, we used these data to describe the time-adjustment in the amplitude of the motor unit force twitches for both the VL and the FDI muscles in the simulation model. The amplitude of each of the individual motor unit force twitches is linearly increased at the beginning of the contraction series (up to 40 s in the VL and 60 s in the FDI) and subsequently decreased to the endurance limit. The slopes of the amplitude increase and decrease are chosen to provide time-dependent changes in the amplitude of the simulated whole muscle force twitch that resemble those obtained empirically. For the VL muscle, we also imposed the condition that the potentiation reaches its maximum at 40 s and returns back to the precontraction value by the end of the first contraction (at 60 s), based on our empirical evidence (see Fig. 8, *bottom*). This constraint was not necessary in the case of the FDI muscle, where the empirical muscle force-twitch amplitude showed slower decrease.

Note that the same slope for the time-dependent increase and decrease in force twitch amplitude was used for all active motor units. The study of Carpentier et al. (2001), where the amplitude of the force twitch increased for earlier-recruited motor units and decreased for later-recruited motor units during the same protocol of repeated contractions at 50% MVC, suggests that later-recruited motor units might actually display faster adjustments in their twitch amplitude. However, we currently lack accurate information to model the time-dependent adjustment of the twitch amplitude for individual motor units as a function of their recruitment threshold during the tracking tasks investigated in this study. However, note that a faster decrease in the force twitch amplitude of later-recruited motor units would not modify the behavioral pattern predicted by the model. It would only accelerate the increase in motor unit firing rate and the recruitment of additional motor units.

Sensitivity test. Also note that in the model, the same changes in the amplitude of the force twitches are applied in a coordinated manner to all active motor units: the amplitude increases only in first 40 s (VL) or 60 s (FDI) and decreases afterward. Thus only motor units recruited in the first 40 or 60 s will actually display potentiation. This assumption is based on the lack of data describing the different changes in twitch amplitude for individual motor units during voluntary isometric contractions, as previously discussed. However, we investigate here a different scenario, simulating the series of repeated contractions presented in Fig. 7 for the FDI muscle by applying the same pattern of force change to all active motor units as a function of the individual motor unit's activation time, instead of as a function of contraction time. Thus the twitch amplitude of all motor units will potentiate in the first 40 or 60 s of their individual activation time and subsequently decrease, irrespectively of when the motor units are recruited in the series of repeated contractions.

The results of this simulation are shown in Fig. A1. Data are presented in a similar manner as in Fig. 7. The resultant excitation, force, and motor unit behavior appears to be qualitatively similar to that of the simulation reported in Fig. 7. During the 20% MVC plateau region of the first contraction, the input excitation required to maintain the target force decreased slightly, leading to decreasing firing rates of the active motor units and derecruitment of several motor units. Adjustments occurred concurrently with an increase in the muscle force twitch amplitude. Throughout the series of repeated contractions, the input excitation needed to exert both the initial 50% MVC and subsequent 20% MVC force increased progressively with contraction time, leading to a progressively greater number of active motor units and to an increase in their firing rates. These adjustments were accompanied by a progressive decrease in the muscle force twitch amplitude and are presented in Fig. A1 and Table A2 for the first and last contraction of the series. The coefficient of variation of the force increased with contraction time. The main differences between the simulation presented here and the one presented in Fig. 7 are *1*) the endurance limit increases when all motor units potentiate during the first minute of their individual activation time (34 sequential contractions were simulated of than 14); *2*) the change in motor unit firing rates during each contraction of the series is less pronounced because the muscle fatigues more gradually; *3*) in each contraction, the last recruited motor unit displays a steady firing rate only after a few seconds of its first recruitment; and *4*) the force fluctuations are higher at the endurance limit due to potentiation of the newly recruited high-threshold high-amplitude force twitch motor units. Note that this simulation is meant to investigate the firing rate behavior of motor units under a plausible alternative time pattern of

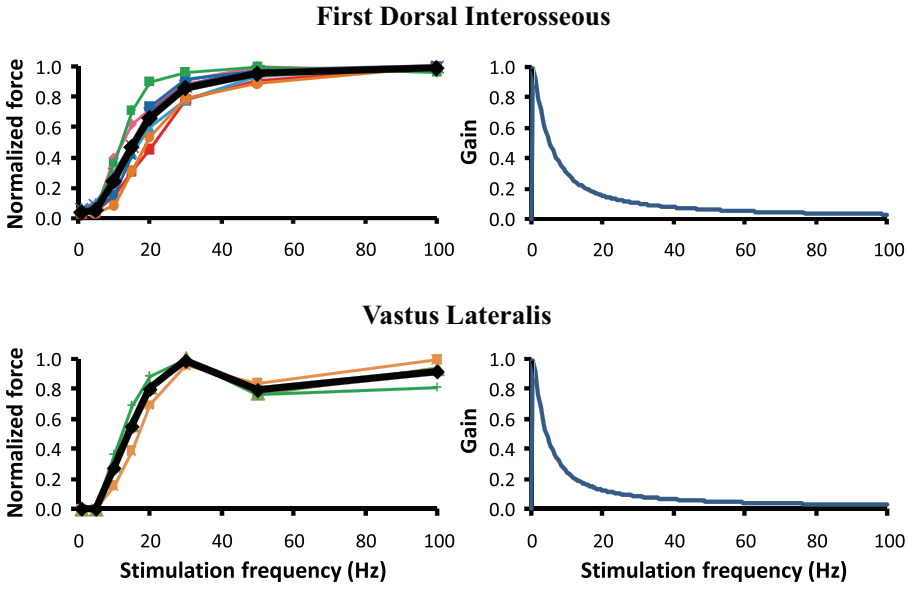

Fig. A3. *Left*: force-frequency relations obtained from previously performed experiment in the FDI of 6 subjects (*top*) and in the VL muscle of 3 subjects (*bottom*). Colored lines represent individual subjects; black line indicates the averaged data. *Right*: firing rate-dependent gain function calculated for the 2 muscles from the fitted force-frequency curves and *Eqs. 13–14*.

the motor unit force twitches. A more realistic appraisal awaits empirical data.

Since we did not find conclusive data on the changes in the time duration of the motor unit force twitch, either from the literature or from our own data, Tr and Thr were maintained constant in the model, a characteristic that can also be improved as more accurate data are made available. However, given the number of disparate reports on this matter that can be found in the literature, we investigate here the behavior of the model when the duration of the motor unit twitches varies in conjunction with the amplitude. Specifically, we simulated the protocol of repeated intermittent force contractions presented in Fig. 7 for the FDI muscle, with the additional constraint that both the rise time and the half-relaxation time of all active motor units either decrease by one-half or double by the endurance limit.

The results of the simulations are presented in Table A3 and are shown in Fig. A2*A* for decreasing force twitch duration and in Fig. A2*B* for increasing force twitch duration over time. Data are presented in a similar manner as in Fig. 7. Again, the resultant excitation, force, and motor unit behavior appears to be qualitatively similar to that of the simulation reported in Fig. 7. The main differences between the simulation presented here and the one presented in Fig. 7 are *1*) the endurance limit decreases when the twitch duration shortens over time (12 sequential contractions were simulated instead of 14), and it increases when the twitch duration lengthens with time (16 sequential contractions instead of 14); and *2*) whereas the twitch duration of the individual motor units actually shortens by one-half or doubles by the endurance limit, the duration of the whole muscle force twitch is only mildly affected. The motor unit amplitude decreases in conjunction to the varying twitch duration, and thus the force of the varying-duration motor units comprises a progressively smaller contribution to the muscle force twitch.

APPENDIX E: FIRING RATE-DEPENDENT GAIN FACTOR

The summation of force during tetanic contractions is nonlinear and depends on the stimulation frequency (Bawa and Stein 1976; Cooper and Eccles 1930; Fuglevand et al. 1993; Mannard and Stein 1973). The relationship between isometric force and stimulus rate has a well-known sigmoidal shape (Bigland and Lippold 1954; Rack and Westbury 1969), which depends on the contractile properties of the motor units. However, if the stimulus rate is normalized as a function of the twitch rise time, the shape of the force-frequency relation is similar for all motor units (Kernell et al. 1983; Thomas et al. 1991b). Furthermore, for normalized stimulus rate lower than 0.4, the gain is almost constant and is similar to that of an isolated twitch (Burke 1981). The nonlinearity was introduced in the model by scaling the impulse trains of each motor unit with a gain factor, which depends on the firing rate of the motor unit.

In our previous experiment, the FDI and the VL muscles were electrically stimulated at supramaximal intensity and increasing rates (1, 5, 10, 15, 20, 30, 50, and 100 Hz), and the twitch response was recorded. The protocol was administered to three subjects in the VL and to seven subjects in the FDI. For details on the VL experiments see Adam and De Luca (2003, 2005). The experimentally obtained force-frequency curves were fitted to the following exponential function (Adam 2003; Herbert and Gandevia 1999; Studer et al. 1999) for normalized stimulus rates (fn) higher than 0.4:

$$y(\mathrm{fn}) = 1 - re^{\frac{(0.4-\mathrm{fn})}{c}}. \qquad (13)$$

The equation was normalized to 1 at the stimulus rate fn = 0.4 and divided by the normalized stimulus rate. The gain factor that accounts for the nonlinear summation of twitches was then evaluated by using the formula:

$$g_{ij}(\mathrm{fn}) = \begin{cases} 1 & 0 < \mathrm{fn}_{ij} \le 4 \\ \dfrac{0.4}{\mathrm{fn}_{ij}(1-r)}\left[1 - re^{\frac{(0.4-\mathrm{fn})}{c}}\right] & \mathrm{fn} > 4 \end{cases} \qquad (14)$$

where g_{ij} is the gain assigned to the jth firing of motor unit i and fn_{ij} is the normalized instantaneous firing rate; $\mathrm{fn}_{ij} = \mathrm{Tr}_i/\mathrm{IPI}_j$ (Tr_i indicates the rise time of motor unit i, IPI_j indicates the jth interpulse interval). The parameter values obtained from the fit of the experimental data are r = 0.87 and c = 2.82 for the FDI muscle and r = 0.85 and c = 2.13 for the VL muscle.

The gain factor is used to scale the amplitude of each motor unit pulse in the train of firings as a function of the corresponding IPI. The force-frequency relation fitted from the experimental data depicted in Fig. A3 for the VL and FDI muscles.

ACKNOWLEDGMENTS

We are grateful to Dr. A. Adam for participating in the preliminary work on the simulation model. This work was done, in part, while P. Contessa was a doctoral candidate in the Bioengineering Curriculum at the School of Information Engineering at the University of Padua (Padua, Italy). We thank Dr. Claudio Cobelli for effectuating the collaboration.

GRANTS

This work was supported in part by National Institutes of Health (NIH) Grant NS-058250 to Altec Inc. for the development of the decomposition system; by National Center for Medical Rehabilitation Research NIH Grant HD-050111; by a grant from the Italian Ministero dell'Università e della Ricerca; and by a grant from Fondazione Ing. A. Gini.

DISCLOSURES

No conflicts of interest, financial or otherwise, are declared by the authors.

AUTHOR CONTRIBUTIONS

P.C. and C.J.D. conception and design of research; P.C. performed experiments; P.C. analyzed data; P.C. and C.J.D. interpreted results of experiments; P.C. prepared figures; P.C. drafted manuscript; P.C. and C.J.D. edited and revised manuscript; P.C. and C.J.D. approved final version of manuscript.

REFERENCES

Adam A. *Control of Motor Units During Submaximal Fatiguing Contractions* (PhD thesis). Boston, MA: Boston University, 2003.

Adam A, De Luca CJ. Recruitment order of motor units in human vastus lateralis muscle is maintained during fatiguing contractions. *J Neurophysiol* 90: 2919–2927, 2003.

Adam A, De Luca CJ. Firing rates of motor units in human vastus lateralis muscle during fatiguing isometric contractions. *J Appl Physiol* 99: 268–280, 2005.

Basmajian JV, De Luca CJ. *Muscles Alive* (5th ed.). Baltimore, MD: Williams and Wilkins, 1985.

Bawa P, Stein RB. Frequency response of human soleus muscle. *J Neurophysiol* 39: 788–793, 1976.

Bellemare F, Woods JJ, Johansson R, Bigland-Ritchie B. Motor-unit discharge rates in maximal voluntary contractions of three human muscles. *J Neurophysiol* 50: 1380–1392, 1983.

Bigland B, Lippold OC. Motor unit activity in the voluntary contraction of human muscle. *J Physiol* 125: 322–335, 1954.

Bigland-Ritchie B, Johansson R, Lippold OCJ, Woods JJ. Contractile speed and EMG changes during fatigue of sustained maximal voluntary contractions. *J Neurophysiol* 50: 313–324, 1983.

Bigland-Ritchie B, Cafarelli E, Vøllestad NK. Fatigue of submaximal static contractions. *Acta Physiol Scand* 128: 137–148, 1986.

Binder-MacLeod SA, McDermond LR. Changes in the force-frequency relationship of the human quadriceps femoris muscle following electrically and voluntarily induced fatigue. *Phys Ther* 72: 95–104, 1993.

Broman H, De Luca CJ, Mambrito B. Motor unit recruitment and firing rates interaction in the control of human muscles. *Brain Res* 337: 311–319, 1985.

Burke RE. Motor unit types of cat triceps surae muscle. *J Physiol* 193: 141–160, 1967.

Burke RE. Motor units: anatomy, physiology, and functional organization. In: *Handbook of Physiology. The Nervous System. Motor Control*. Bethesda, MD: Am. Physiol. Soc., 1981, p. 345–422.

Burke RE, Levine DN, Tsairis P, Zajac FE. Physiological types and histochemical profiles in motor units of the cat gastrocnemius. *J Physiol* 234: 723–748, 1973.

Calancie B, Bawa P. Voluntary and reflexive recruitment of flexor carpi radialis motor units in humans. *J Neurophysiol* 53: 1194–1200, 1985.

Carpentier A, Duchateau J, Hainaut K. Motor unit behaviour and contractile changes during fatigue in the human first dorsal interosseous. *J Physiol* 534: 903–912, 2001.

Christensen E. Topography of terminal motor innervation in striated muscles from stillborn infants. *Am J Phys Med* 38: 65–78, 1959.

Christova P, Kossev A. Human motor unit recruitment and derecruitment during long lasting intermittent contractions. *J Electromyogr Kinesiol* 11: 189–196, 2001.

Clamann HP. Statistical analysis of motor unit firing patterns in a human skeletal muscle. *Biophys J* 9: 1233–1251, 1969.

Contessa P, Adam A, De Luca CJ. Motor unit control and force fluctuation during fatigue. *J Appl Physiol* 107: 235–243, 2009.

Cooper S, Eccles JC. The isometric responses of mammalian muscles. *J Physiol* 69: 377–385, 1930.

De Luca CJ. Physiology and mathematics of myoelectric signals. *IEEE Trans Biomed Eng* 26: 313–325, 1979.

De Luca CJ. How are the motor units controlled to regulate force? *Proceedings of the 1995 Myoelectric Controls/Powered Prosthetics Symposium, New Brunswick, Canada*, August 1995.

De Luca CJ, Contessa P. Hierarchical control of motor units in voluntary contraction. *J Neurophysiol* 107: 178–195, 2012.

De Luca CJ, Erim Z. Common drive of motor units in regulation of muscle force. *Trends Neurosci* 17: 299–305, 1994.

De Luca CJ, Forrest WJ. Some properties of motor unit action potential trains recorded during constant force isometric contractions in man. *Kybernetik* 12: 160–168, 1973.

De Luca CJ, Hostage EC. Relationship between firing rate and recruitment threshold of motoneurons in voluntary isometric contractions. *J Neurophysiol* 104: 1034–1046, 2010.

De Luca CJ, Kline JC. Influence of proprioceptive feedback on the firing rate and recruitment of motoneurons. *J Neural Eng* 9: 016007, 2012.

De Luca CJ, Adam A, Wotiz R. Decomposition of surface EMG signals. *J Neurophysiol* 96: 1646–1657, 2006.

De Luca CJ, Foley PJ, Erim Z. Motor unit control properties in constant-force isometric contractions. *J Neurophysiol* 76: 1503–1516, 1996.

De Luca CJ, Gonzalez-Cueto JA, Adam A. Motor unit recruitment and proprioceptive feedback decrease the common drive. *J Neurophysiol* 101: 1620–1628, 2008.

De Luca CJ, LeFever RS, McCue MP, Xenakis AP. Behaviour of human motor units in different muscles during linearly varying contractions. *J Physiol* 329: 113–128, 1982a.

De Luca CJ, LeFever RS, McCue MP, Xenakis AP. Control scheme governing concurrently active human motor units during voluntary contractions. *J Physiol* 329: 129–142, 1982b.

De Ruiter CJ, Elzinga MJ, Verdijk PW, van Mechelen W, de Haan A. Voluntary drive-dependent changes in vastus lateralis motor unit firing rates during a sustained isometric contraction at 50% of maximum knee extension force. *Pflügers Arch* 447: 436–444, 2004.

Dideriksen JL, Farina D, Baekgaard M, Enoka RM. An integrative model of motor unit activity during sustained submaximal contractions. *J Appl Physiol* 108: 1550–1562, 2010.

Dideriksen JL, Farina D, Enoka RM. Neuromuscular adjustments that constrain submaximal EMG amplitude at task failure of sustained isometric contractions. *J Appl Physiol* 111: 485–494, 2011.

Dolmage T, Cafarelli E. Rate of fatigue during repeated submaximal contractions of human quadriceps muscle. *Can J Physiol Pharmacol* 69: 1410–1415, 1991.

Dorfman LJ, Howard JE, McGill KC. Triphasic behavior response of motor units to submaximal fatiguing exercises. *Muscle Nerve* 13: 621–628, 1990.

Duchateau J, Hainaut K. Effects of immobilization on contractile properties, recruitment and firing rates of human motor units. *J Physiol* 422: 55–65, 1990.

Eccles JC, Eccles RM, Lundberg A. The action potentials of the alpha motoneurons supplying fast and slow muscles. *J Physiol* 142: 275–291, 1958.

Elek JM, Dengler R. Human motor units studied by intramuscular microstimulation. In: *Fatigue*, edited by Gandevia SC, Enoka RM, McComas AJ, Stuart DG, Thomas CK. New York: Plenum, 1995, p. 161–171.

Elek JM, Kossev A, Dengler R, Schubert M, Wholfahrt K, Wolf W. Parameters of human motor unit twitches obtained by intramuscular microstimulation. *Neuromuscul Disord* 2: 261–267, 1992.

Erim Z, De Luca CJ, Mineo K, Aoki T. Rank-ordered regulation of motor units. *Muscle Nerve* 19: 563–573, 1996.

Feiereisen P, Duchateau J, Hainaut K. Motor unit recruitment order during voluntary and electrically induced contractions in the tibialis anterior. *Exp Brain Res* 114: 117–123, 1997.

Feinstein B, Lindegård B, Nyman E, Wohlfart G. Morphologic studies of motor units in normal human muscles. *Acta Anat (Basel)* 23: 127–142, 1955.

Fuglevand AJ, Macefield VG, Bigland-Ritchie B. Force-frequency and fatigue properties of motor units in muscles that control digits of the human hand. *J Neurophysiol* 81: 1718–1729, 1999.

Fuglevand AJ, Winter DA, Patla AE. Models of recruitment and rate coding organization in motor-unit pools. *J Neurophysiol* 70: 2470–2488, 1993.

Furness P, Jessop J, Lippold OCJ. Long-lasting increases in the tremor of human hand muscles following brief, strong effort. *J Physiol* 265: 821–831, 1977.

Garland SJ, Enoka RM, Serrano LP, Robinson GA. Behavior of motor units in human biceps brachii during a submaximal fatiguing contraction. *J Appl Physiol* 76: 2411–2419, 1994.

Garland SJ, Griffin L, Ivanova T. Motor unit discharge rate is not associated with muscle relaxation time in sustained submaximal contractions in humans. *Neurosci Lett* 239: 25–28, 1997.

Gorassini M, Yang JF, Siu M, Bennett DJ. Intrinsic activation of human motoneurons: possible contribution to motor unit excitation. *J Neurophysiol* 87: 1850–1858, 2002a.

Gorassini M, Yang JF, Siu M, Bennett DJ. Intrinsic activation of human motoneurons: reduction of motor unit recruitment threshold by repeated contractions. *J Neurophysiol* 87: 1859–1866, 2002b.

Gossen ER, Ivanova TD, Garland SJ. The time course of the motoneuron afterhyperpolarization is related to motor unit twitch speed in human skeletal muscle. *J Physiol* 552: 657–664, 2003.

Henneman E, Olson CB. Relation between structure and function in the design of skeletal muscles. *J Neurophysiol* 28: 581–598, 1965.

Herbert RD, Gandevia SC. Twitch interpolation in human muscles: mechanisms and implications for measurement of voluntary activation. *J Neurophysiol* 82: 2271–2283, 1999.

Kernell D. The adaptation and relation between discharge frequency and current strength of cat lumbosacral motoneurons stimulated by long-lasting injected currents. *Acta Physiol Scand* 65: 65–73, 1965a.

Kernell D. The limits of firing frequency in cat lumbosacral motoneurones possessing different time course of afterhyperpolarization. *Acta Physiol Scand* 65: 87–100, 1965b.

Kernell D, Ducati A, Sjöholm H. Properties of motor units in the first deep lumbrical muscle of the cat's foot. *Brain Res* 98: 37–55, 1975.

Kernell D, Eerbeek O, Verhey BA. Relation between isometric force and stimulus rate in cat's hindlimb motor units of different twitch contraction times. *Exp Brain Res* 50: 220–227, 1983.

Kossev A, Elek JM, Schubert M, Dengler R, Wolf W. Assessment of human motor unit twitches—a comparison of spike-triggered averaging and intramuscular microstimulation. *Electroencephalogr Clin Neurophysiol* 93: 100–105, 1994.

Kuchinad RA, Ivanova TD, Garland SJ. Modulation of motor unit discharge rate and H-reflex amplitude during submaximal fatigue of the human soleus muscle. *Exp Brain Res* 158: 345–355, 2004.

Lowery MM, Erim Z. A simulation study to examine the effect of common motoneuron inputs on correlated patterns of motor unit discharge. *J Comput Neurosci* 19: 107–124, 2005.

Lüscher HR, Ruenzel P, Henneman E. How the size of motoneurons determines their susceptibility to discharge. *Nature* 282: 859–861, 1979.

Macefield VG, Fuglevand AG, Howell JN, Bigland-Ritchie B. Discharge behavior of single motor units during maximal voluntary contractions of a human toe extensor. *J Physiol* 528: 227–234, 2000.

Macintosh BR, Grange RW, Cory CR, Houston ME. Contractile properties of rat gastrocnemius muscle during staircase fatigue and recovery. *Exp Physiol* 79: 59–70, 1994.

Mannard A, Stein RB. Determination of the frequency response of isometric soleus muscle in the cat using random nerve stimulation. *J Physiol* 229: 275–296, 1973.

Marsden CD, Meadows JC, Merton PA. "Muscular Wisdom" that minimizes fatigue during prolonged effort in man: peak rates of motoneuron discharge and slowing of discharge during fatigue. *Adv Neurol* 39: 169–211, 1983.

Maton B, Gamet D. The fatigability of two agonistic muscles in human isometric voluntary contraction: an EMG study. II. Motor unit firing rate and recruitment. *Eur J Appl Physiol* 58: 369–374, 1989.

McNulty PA, Falland KJ, Macefield VG. Comparison of contractile properties of single motor units in human intrinsic and extrinsic finger muscles. *J Physiol* 526: 445–456, 2000.

Mendell LM, Henneman E. Terminals of single Ia fibers: distribution within a pool of 300 homonymous motor neurons. *Science* 160: 96–98, 1968.

Milner-Brown HS, Stein RB, Yemm R. The orderly recruitment of human motor units during voluntary isometric contractions. *J Physiol* 230: 359–370, 1973.

Monster AW, Chan H. Isometric force production by motor units of extensor digitorum communis muscle in man. *J Neurophysiol* 40: 1432–1443, 1977.

Moritz CT, Barry BK, Pascoe MA, Enoka RM. Discharge rate variability influences the variation in force fluctuations across the working range of a hand muscle. *J Neurophysiol* 93: 2449–2459, 2005.

Nawab SH, Chang SS, De Luca CJ. High-yield decomposition of surface EMG signals. *Clin Neurophysiol* 121: 1602–1615, 2010.

Nordstrom MA, Fuglevand AJ, Enoka ME. Estimating the strength of common input to human motoneurons from the cross-correlogram. *J Physiol* 453: 547–574, 1992.

Person RS, Kudina LP. Discharge frequency and discharge pattern of human motor units during voluntary contraction of muscle. *Electroencephalogr Clin Neurophysiol* 32: 471–483, 1972.

Powers RK, ElBasiouny SM, Rymer WZ, Heckman CJ. Contribution of intrinsic properties and synaptic inputs to motoneuron discharge patterns: a simulation study. *J Neurophysiol* 107: 808–823, 2012.

Rack PMH, Westbury DR. The effects of length and stimulus rate on tension in the isometric cat soleus muscle. *J Physiol* 204: 443–460, 1969.

Raikova TR, Aladjov HT. Hierarchical genetic algorithm versus static optimization—investigation of elbow flexion and extension movements. *J Biomech* 35: 1123–1135, 2002.

Shimizu T. Motor unit activities of human masseter muscle during sustained voluntary contractions [in Japanese]. *Nihon Hotetsu Shika Gakkai Zasshi* 34: 115–127, 1990.

Slifkin AB, Vaillancourt DE, Newell KM. Intermittency in the control of continuous force production. *J Neurophysiol* 84: 1708–1718, 2000.

Stephens JA, Usherwood TP. The mechanical properties of human motor units with special reference to their fatigability and recruitment. *Brain Res* 125: 91–97, 1977.

Studer LM, Ruegg DG, Gabriel JP. A model for steady isometric muscle activation. *Biol Cybern* 80: 339–355, 1999.

Taylor AM, Steege GW, Enoka RM. Motor unit synchronization alters spike triggered average force in simulated contractions. *J Neurophysiol* 88: 265–276, 2002.

Thomas CK, Del Valle A. The role of motor unit rate modulation versus recruitment in repeated submaximal voluntary contractions performed by control and spinal cord injured subjects. *J Electromyogr Kinesiol* 11: 217–229, 2001.

Thomas CK, Bigland-Ritchie B, Westling G, Johansson RS. A comparison of human thenar motor-unit properties studied by intraneural motor-axon stimulation and spike-triggered averaging. *J Neurophysiol* 64: 1347–1351, 1990.

Thomas CK, Johansson RS, Bigland-Ritchie B. Attempts to physiologically classify human thenar motor units. *J Neurophysiol* 65: 1501–1508, 1991a.

Thomas CK, Bigland-Ritchie B, Johansson RS. Force-frequency relation of human thenar motor units. *J Neurophysiol* 65: 1509–1516, 1991b.

Thomas CK, Ross BH, Stein RB. Motor-unit recruitment in human first dorsal interosseous muscle for static contractions in three different directions. *J Neurophysiol* 55: 1017–1029, 1986.

Vandervoort AA, Quinlan J, McComas AJ. Twitch potentiation after voluntary contraction. *Exp Neurol* 81: 141–152, 1983.

Vøllestad NK, Sejersted I, Saugen E. Mechanical behavior of skeletal muscle during intermittent voluntary isometric contractions in humans. *J Appl Physiol* 83: 1557–1565, 1997.

Yao W, Fuglevand AJ, Enoka RM. Motor-unit synchronization increases EMG amplitude and decreases force steadiness of simulated contractions. *J Neurophysiol* 83: 441–452, 2000.

Young JL, Meyer RF. Physiological properties and classification of single motor units activated by intramuscular microstimulation in the first dorsal interosseous muscle in man. In: *Motor Unit Types Recruitment and Plasticity in Health and Disease*, edited by Desmedt JE. Basel, Switzerland: Karger, 1981, p. 17–25.

Zhou P, Rymer WZ. Factors governing the form of the relation between muscle force and the EMG: a simulation study. *J Neurophysiol* 92: 2878–2886, 2004.

Zhou P, Suresh NL, Rymer ZW. Model based sensitivity analysis of EMG-force relation with respect to motor unit properties: applications to muscle paresis in stroke. *Ann Biomed Eng* 35: 1521–1531. 2007.